Estudios Geológicos
enero-junio 2023, 79(1), e152
ISSN-L: 0367-0449
https://doi.org/10.3989/egeol.44880.624

Ostracods of the Cenomanian-Turonian transition in the Ksour and Amour Mountains (Saharan Atlas, Algeria): systematic and palaeobiogeographic implications

Ostrácodos del tránsito Cenomaniense-Turoniense en los Montes Ksour y Amour (Atlas Sahariano): sistemática e implicaciones paleobiogeográficas

Mustapha Benadla[1], Abbas Marok[1], Choukri Soulimane[1], Matías Reolid[2,*]

[1] Department of Earth and Universe Sciences, University of Tlemcen, P.O. Box 119 Tlemcen, Algeria. ORCID ID: https://orcid.org/0009-0006-3047-1390, https://orcid.org/0000-0001-9119-9198, https://orcid.org/0000-0001-9084-6285
[2] Departamento de Geología, Universidad de Jaén, Campus Las Lagunillas sn, 23071 Jaén, Spain. ORCID ID: https://orcid.org/0000-0003-4211-3946
*Corresponding author: mreolid@ujaen.es

ABSTRACT

The study of ostracods from the Cenomanian-Turonian transition in the Ksour and Amour Mountains (Saharan Atlas, Algeria) has allowed the identification of fossil assemblages characterising this relevant time interval characterised by global environmental changes. The ostracod assemblages consist of fifteen species and seven genera, and are dominated by the Family Cytherellidae (mainly genus *Cytherella*), and secondarily by the families Paracyprididae (exclusively *Paracypris*) and Trachyleberididae (mainly *Cythereis*). Less common are components of families Bairdiidae, Bythocypridae and Macrocyprididae. The studied ostracod assemblages were compared with those assemblages from basins belonging to palaeobiogeographic provinces of North Africa-Middle East (Gondwana Palaeomargin) to search for possible similarities among basins. Thus, the results obtained show the proximity of the ostracod fauna of the Moroccan and Egyptian basins, to which the two basins belonging to the Middle East (Jordan and Oman) are related, the strong similarity between the basins of the Saharan Atlas (Algeria and Tunisia) and finally, the isolation of the ostracod fauna of the Lebanese Basin. This palaeobiogeographical topology shows the probable existence of communication routes during the Cenomanian-Turonian transition or equivalent palaeoenvironmental conditions in different basins.

Keywords: Ostracoda; Upper Cretaceous; North Gondwana Palaeomargin; Palaeobiogeography; Similarity

RESUMEN

El estudio de los ostrácodos de la transición Cenomaniense-Turoniense (Cretácico superior) en los Montes Ksour y Monte Amour (Atlas Sahariano, Argelia) ha permitido la identificación de asociaciones fósiles típicas de este periodo caracterizado por cambios ambientales a escala global. La asociacion de ostrácodos consiste en

Recibido el 14 de noviembre de 2022; Aceptado el 7 de marzo de 2023; Publicado online el 10 de mayo de 2023

Citation / Cómo citar este artículo: Benadla, M., et al. (2022) Ostracods of the Cenomanian-Turonian transition in the Ksour and Amour Mountains (Saharan Atlas, Algeria): systematic and palaeobiogeographic implications. Estudios Geológicos 79(1): e152. https://doi.org/10.3989/egeol.44880.624

15 especies y 7 géneros, y se encuentra dominada por la familia Cytherellidae (principalmente el género *Cytherella*), y en menor medida por las familias Paracyprididae (exclusivamente *Paracypris*) y Trachyleberididae (principalmente *Cythereis*). Las formas menos comunes corresponden a las familias Bairdiidae, Bythocypridae y Macrocyprididae. Las asociaciones de ostrácodos del Atlas Sahariano fueron comparadas con las asociaciones de cuencas vecinas pertenecientes a la provincia paleobiogeográfica del Norte de África y Oriente Medio (margen septentrional de Gondwana) con el fin de encontrar similitudes entre cuencas. Así, el resultado obtenido muestra una gran similitud entre la fauna de ostrácodos de las cuencas del Atlas Sahariano en Argelia y Túnez. Por otro lado, existe similaridad entre las asociaciones de las cuencas de Marruecos y Egipto, y de ambas a su vez con las cuencas de Oriente Medio (Jordán y Omán). Finalmente, la fauna de la Cuenca Libanesa aparece relativamente aislada. Estas similaridades entre distintas cuencas desde el punto de vista palaeobiogeográfico pueden evidenciar cierta comunicación entre las mismas o condiciones ambientales equivalentes durante el tránsito Cenomaniense-Turoniense.

Palabras clave: Ostrácodos; Cretácico superior; Paleomargen septentrional de Gondwana; Paleobiogeografía; Similaridad

Introduction

The Cenomanian–Turonian transition was marked by palaeoceanographic and palaeoclimatic perturbations related to long-lasting carbon isotope anomalies and to an oceanic anoxic event (OAE2; Jenkyns, 1980, 1997; Schlanger *et al*., 1987; Jarvis *et al*., 1988; Robaszynski, 1989; Kaiho & Hasegawa, 1994; Erbacher & Thurow, 1997; Huber *et al*., 2002; Friedrich *et al*., 2006; Turgeon & Creaser, 2008; Voigt *et al*., 2008; Gebhardt *et al*., 2010; Monteiro *et al*., 2012; Erba *et al*., 2013; Elderbak *et al*., 2014; Reolid *et al*., 2016).

In North Africa-Middle East, these both bioevent and isotopic event have widely been studied in Morocco (e.g. Gebhardt *et al*., 2004, 2010; Ettachfini & Andreu, 2004; Ettachfini *et al*., 2005; Ettachfini, 2006; Jati *et al*., 2010; Lézin *et al*., 2012; Prauss, 2012; Andreu *et al*., 2013; Aquit *et al*., 2013; Wang *et al*., 2021), in Algeria (e.g. Naili *et al*., 1995; Harket & Delfaud, 2000, Grosheny *et al*., 2008, 2013; Ruault-Djerrab *et al*., 2012, 2014, Benadla *et al*., 2018), in Tunisia (e.g. Accarie *et al*., 2000; Amédro *et al*., 2005; Caron *et al*., 2006; Zagrarni *et al*., 2008; Robaszynski *et al*., 2010; Negra *et al*., 2011, Grosheny *et al*., 2013; Zaghbib-Turki & Soua, 2013; Reolid *et al*., 2015; Aguado *et al*., 2016; Touir *et al*., 2017), in Egypt (e.g. Lüning *et al*., 1998; Aly *et al*., 2001; Bauer *et al*., 2002; Zakhera & Kassab, 2002; Ismail *et al*., 2009; Nagm, 2009; Gertsch *et al*., 2010; Nagm *et al*., 2010; El-Sabbagh *et al*., 2011; Ayoub-Hannaa *et al.,* 2013; Shahin & Elbaz*,* 2013a; Wilmsen & Nagm, 2013; Nagm *et al*., 2021), in Jordan (e.g. Schulze *et al*., 2004; Aly *et al*., 2008; Morsi & Wendler, 2010; Wendler *et al*., 2010; Bergue *et al*., 2016; Nagm *et al*., 2017; Momani, 2021) and in Oman (Athersuch, 1988).

The OAE2 has been associated to climatic and palaeoceanographic changes including a sea-level transgression (Hallam, 1992), a perturbation of the carbon cycle (e.g. Kuypers *et al*., 2002; Erba, 2004; Pogge von Strandmann *et al*., 2013), a greenhouse warming (e.g. Huber *et al*., 2002; Norris *et al*., 2002; Pogge von Strandmann *et al*., 2013), and a probable massive magmatic episode (e.g. Kuroda *et al*., 2007; Turgeon & Creaser, 2008; Erba *et al*., 2013). The impact of this event on fossil assemblages have been focused on different groups of organisms such as cephalopods (e.g. Monnet, 2009; Nagm *et al*., 2017; Kostak *et al*., 2018), bivalves (e.g. Takahashi, 2005; Negra *et al*., 2011; Posenato *et al*., 2020), foraminifera (e.g. Gebhardt *et al*., 2004; Caron *et al*., 2006; Friedrich *et al*., 2006; Ismail *et al*., 2009; Elderbak *et al*., 2014; Reolid *et al*., 2015, 2016; Bryant & Belanger, 2023) and nannoplankton (e.g. Wan *et al*., 2003; Hardas & Mutterlose, 2007; Erba *et al*., 2013; Aguado *et al*., 2016; Farouk *et al*., 2022). However, recent studies on ostracod assemblages from Cenomanian-Turonian transition are comparatively scarcer (Horne *et al*., 2011; Andreu *et al*., 2013; Benadla *et al*., 2018; Khalil, 2020; Shahin & Elbaz, 2013b; Mebarki *et al*., 2016; Tchenar *et al*., 2020).

The purpose of this present work is to study the ostracods of the Cenomanian-Turonian transition in the Ksour and Amour Mountains (Saharan Atlas, Algeria). It is a systematic and palaeobiogeographic study that allowed us to highlight a global biological event corresponding to the explosion of smooth-shaped ostracods, represented mainly by the Family Cytherellidae (Barroso-Barcenilla *et al*., 2011; Shahin & Elbaz, 2013b; Benadla *et al*., 2018). The biogeographic analysis is carried out to test for the presence of potential similarities between the ostracod assemblages of the Atlasic Basin and other basins of the northern palaeomargin of Gondwana outcropping in the North Africa and the Middle East (Fig. 1).

Geological Setting

The Ksour Mountains (Western Saharan Atlas) and Amour Mountains (Central Saharan Atlas) are part of a vast mountainous area, the Atlas Cordillera, stretching for almost 2000 km from Agadir in Morocco to Gabes in Tunisia. It includes from west to east: the Moroccan High Atlas, the Saharan Atlas, the Aurès and finally the Tunisian Atlas (Fig. 2A). This cordillera presents a general NE-SW orientation. In Algeria, the Saharan Atlas is represented by a structural alignment extending over more than 1000 km, from the Algerian-Moroccan borders in the west to the western limit of the Aurès Mountains in the east. It is composed of the Ksour Mountains, Amour Mountains and the Ouled Naïl Mountains (Fig. 2B). The Zibane and the Aurès follow these clusters. A total of three sections have been studied from Ksour Mountains (Rhoundjaïa, M'Daouer and Chellala Dahrania) and other from Amour Mountains (El Kohol).

Ksour Mountains (Western Saharan Atlas)

Part of the great orographic barrier of the Saharan Atlas, the Ksour Mountains are located approximately 360 km south of Oran. They are limited to the north by the Oran High Plains, to the south by the Saharan platform, to the east by Amour Mountains and finally to the west by the Moroccan High Atlas (Fig. 2B). The Ksour Mountains formed at the location of more or less subsident intra-plate basins (Aït Ouali, 1991; Aït Ouali & Delfaud, 1995) and this sub-basin shows a tectonic style that is more brittle in the west and more flexible in the east. The so-called soft tectonics is represented by narrow anticlines with straightened sides and more or less horizontal

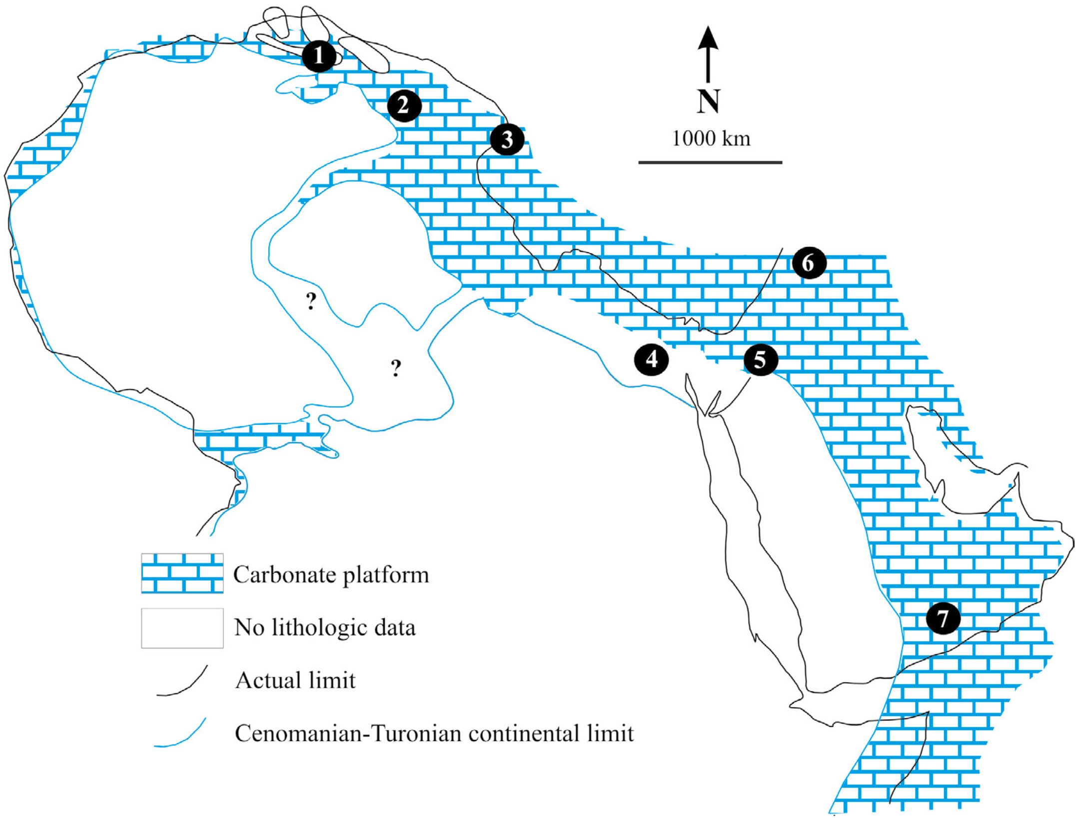

Figure 1.— Geographic location of the analysed regions (After Andreu *et al*., 2013). 1. Morocco, 2. Algeria, 3. Tunisia, 4. Egypt, 5. Jordan, 6. Lebanon, 7. Oman.

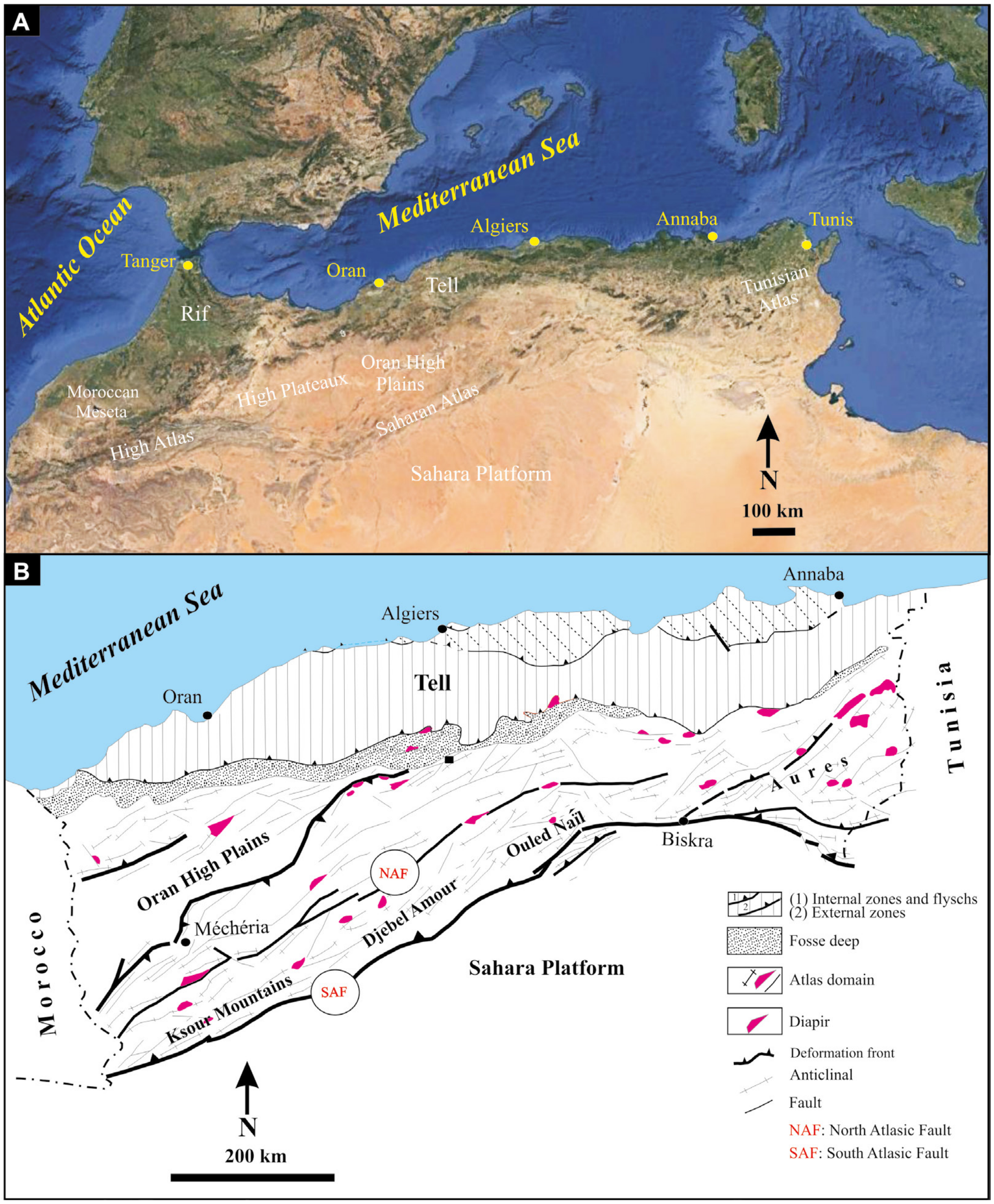

Figure 2.— Geographic and geologic sketch. A) Situation map of the Saharan Atlas, B) Geological map of the area studied.

vaults separating large synclines with generally flat bottoms, wider and more elongated where the Cretaceous terrain is preserved (Yelles-Chaouche *et al*., 2001). It should be noted that the major phase that structured the Ksour Sub-basin in question generated isopaque folds with a SW-NE direction and is dated to the Lutetian-Priabonian (Coiffait *et al*., 1984). Geologically, the filling of the Ksour Sub-basin consists of Triassic and Jurassic rocks, predominantly carbonates (Bassoullet, 1973; Delfaud, 1975; Elmi *et al*., 1998; Mekahli, 1998; Reolid *et al*., 2012). The Lower Cretaceous is constituted by siliciclastic sedimentary rocks (fluvial and deltaic) overlaid by the first marine carbonate deposits attributed to the Upper Cretaceous. Thus, during the Cenomanian a major transgression flooded the Sahara and the Ksour Sub-basin (Busson *et al*., 1999; Grosheny *et al*., 2008, 2013). There are two major sequences in the Upper Cretaceous correlatable at the scale of the Saharan Atlas (Delfaud, 1986; Harket & Delfaud, 2000): CI (Cenomanian-Turonian) and CII (Coniacian to Maastrichtian). According to the geological map of Galmier (1972) and the work of Bassoullet (1973), the Cenomanian and Turonian deposits form the upper level of the Mesozoic folded series. The Cenozoic deposits are essentially continental siliciclastics (sandstones and conglomerates).

Amour Mountains (Central Saharan Atlas)

The Amour Mountains are bounded to the north by the Oran High Plains, to the south by the Saharan platform, to the east by the Ouled Naïl Mountains and to the west by the eastern end of the Ksour Mountains (Fig. 2B). Unlike the Ksour Mountains, this part of the Saharan Atlas is characterised by large synclinal and anticlinal folds (Kazi-Tani, 1986), elongated NE-SW in the western part and E-W in the eastern part (Bettathar, 2009). Furthermore, the so-called brittle tectonics is expressed in this sub-basin by three major N-S, E-W and NW-SE trending faults (Guiraud, 1990). According to Bettahar *et al*. (2007), the evolution of the Amour Sub-basin records several compressive tectonic phases from the Early Cretaceous to the Mio-Pliocene. Geologically, the stratigraphic series of Amour Mountains is formed by a thick sedimentary series covering the Mesozoic-Cenozoic stratigraphic interval. It consists of Triassic gypsum and salt-rich clays, with local doleritic volcanic rocks, overlaid by Jurassic carbonates, marlstones and sandstone-siltstone alternations. The Lower Cretaceous is characterised by limestones and sandstones-silstones rich in gypsum and claystones, whereas the Upper Cretaceous is constituted by dolomitic limestones, gypsum-rich marls and marly-limestone alternations (Guillemot & Estorges, 1981; Abed, 1982; Kazi-Tani, 1986; Bracene, 2001; Bettahar, 2009; Zazoun *et al*., 2015). The Cenozoic is represented mainly by continental siliciclastic deposits.

Material and Methods

The chronological interval studied in the different sections, the *Whiteinella archaeocretacea* Zone that contains the Cenomanian-Turonian boundary (see Caron *et al*., 2006; Reolid *et al*., 2015), consists mainly of limestone beds and some marlstone levels. A total of 107 samples have been analyzed (35 from Rhoundjaïa, 18 from M'Daouer, 20 from Chellala Dahrania, and 34 from El Kohol). Most of the samples were from limestones and prepared for thin sections and analysis of microfacies, where as a total of 30 marl samples (500 g/sample) were washed under a gentle jet of water over a set of standard stainless-steel sieves (250 µm, 125 µm and 63 µm) and sorted for examining ostracods and foraminifera. The identification and systematic classification of ostracods is based mainly on the work of Bassoullet & Damotte (1969), Andreu *et al*. (2013) and Benadla (2019). The most systematically and biostratigraphically representative species were selected and gold-coated for analyzing under a scanning electron microscope Merlin Carl Zeiss SEM at the University of Jaén (Centro de Instrumentación Científico-Técnica).

In this work, the application of quantitative biogeography is used to compare the studied ostracod assemblages with those from different basins belonging to different palaeobiogeographic provinces. Therefore, the basins included in the palaeobiogeographic analysis are located in Morocco (Agadir Basin, Central High Atlas, Middle Atlas and Preafrican Basin) (Andreu, 2002; Ettachfini & Andreu, 2004; Ettachfini *et al*., 2005; Jati *et al*., 2010), Algeria (Ksour, Amour and Tébessa sub-basins) (Benadla, 2019; Ruault-Djerrab *et al*, 2012), Tunisia (Central Tunisia) (Salmouna *et al*., 2014), Egypt (East and central Sinai) (El-Nady *et al*., 2008; Shahin & Elbaz, 2013a), Jordan (Central Jordan) (Morsi & Wendler, 2010), Lebanon (Damotte & Saint-Marc, 1972) and finally western Oman (Athersuch, 1988). This biogeographical quantification is based on two types of data processing:

- For the analysis of the quantitative data (abundance), the *PAST*-PAlaeontological *STatistics* software, ver. 1.89 (Hammer *et al*., 2009) was used. In this software, the matrix obtained in terms of number of genera per family for each region (Table 1) is processed using the Principal Coordinates Analysis. The latter is the result of the distance measure based here on the Bray-Curtis coefficient. It should be noted that

the distance calculation algorithm depends on the type of matrix constructed.
- For the processing of qualitative (binary) data, we chose the *BG-Index* ver. 1.1 β software (Escarguel, 2001). This is done with the aim of comparing the degree of similarity or dissimilarity between each pair of lists generated by the database. In this analysis, a degree is calculated by the similarity (Jaccard and Dice coefficients) or distance (Bray-Curtis coefficient) indices. The results of these calculations are represented in the form of a phenogram which will be transformed later into a "Hierarchical Association Diagram".

Lithostratigraphy

As indicated before, the studied ostracod assemblages come from four sections (Fig. 3): Rhoundjaïa and M'Daouer (western Ksour Mountains), Chellala Dahrania (eastern Ksour Mountains) and El Kohol (Amour Mountains).

Rhoundjaïa section

Located at 60 km west of locality of Aïn Séfra, the Rhoundjaïa section (32º44'45.00"N, 0º14'24.58"W) was studied on the south-western end of a SSW-NNE syncline (Fig. 3B). This section is of particular interest for the study of the Cenomanian-Turonian transition (Bassoullet & Damotte, 1969; Galmier, 1972; Bassoullet, 1973; Marok *et al*., 2009; Mebarki *et al*., 2016; Benadla *et al*., 2018). Lithostratigraphically, the two geomorphologically detectable bars (Fig. 4A) correspond to the Rhoundjaïa Formation (58.15 m) which can be subdivided into three members (Fig. 5A):
- Lower Member (24.25 m) overlyes the M'Daouer Formation composed by gypsum-rich

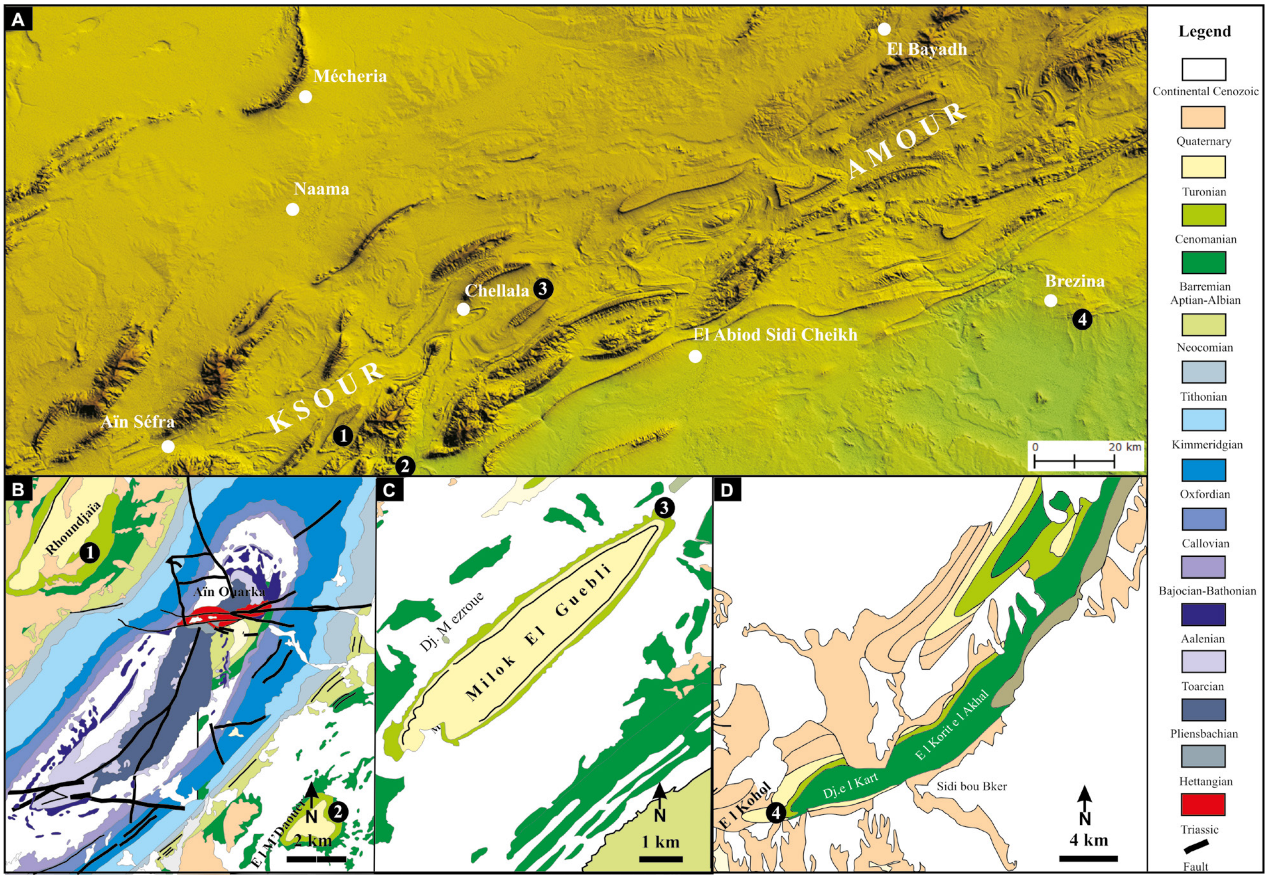

Figure 3.— Geological setting of the studied sections in the Ksour and Amour Mountains (Saharan Atlas). A) Location map of the study sections (1. Rhoundjaïa, 2. M'Daouer, 3. Chellala Dahrania, and 4. El Kohol). B and C), Geological map of the Ksour Mountains. D) Geological map of the Amour Mountains.

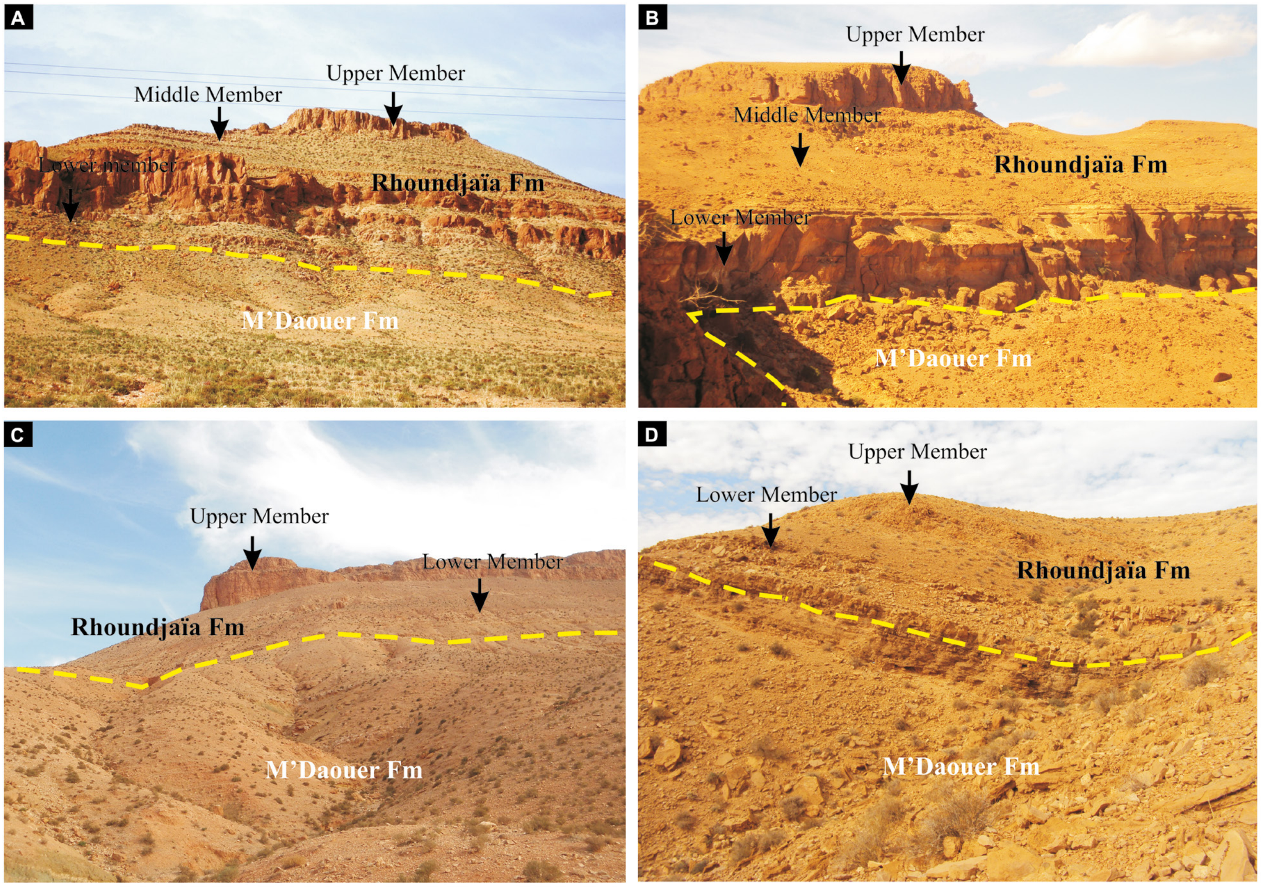

Figure 4.— Outcrop view of studied sections. A. Rhoundjaïa section, B. M'Daouer section, C. Chellala Dahrania section, and D. El Kohol section.

claystones, limestones and dolostones, and this lower member is mainly composed of bioclastic bioturbated limestones (wackestones to packstones of ostracods and planktic foraminifera) with common *Thalassinoides* and *Planolites*. Locally it is recorded mudstone with planktic foraminifera (Benadla *et al*., 2018). In the Lower Member are recorded *Dicarinella* sp., *Rotalipora* sp., *Muricohedbergella delrioensis*, *M. planispira*, *Planoheterohelix moremani*, *Helvetoglobotruncana praehelvetica* and *Guembelitria cretacea*. The genus *Rotalipora* is restricted to the lowermost part of the section (samples Rh-4 and Rh-5) and *Guembelitria* is recorded in the top of the Lower Member (from sample Rh-14) (Benadla *et al*., 2018).

- Middle Member (30 m) is an alternation of whitish bioclastic limestones (wackestones to packstones with foraminifera, filaments and echinoderms) and marls with some lumpy levels rich in sea urchins (*Holaster subglobosus*, *Mecaster pseudofournelli*, *Hemiaster syriacus* and *Prionocidaris granulostriata*), ammonites (*Vascoceras gamai* and *Vascoceras* sp.) and gastropods (*Tylostoma* sp.). Locally, there are dense accumulations of serpulids. The bioturbated carbonate levels correspond to biomicrites. Towards the top, this alternation is followed by limestones with flint nodules and bioturbated limestones with *Thalassinoides*. Planktic foraminiferal assemblage is dominated by *Planoheterohelix moremani*, *P. reussi*, *Guembelitria cretacea* and *G. cenomana*. The species of the genus *Muricohedbergella* are recorded in the lower part of this member.
- Upper Member (10.60 m) is constituted by massive beds of slightly bioclastic (wackestones to packstones of foraminifera, ostracods and fila-

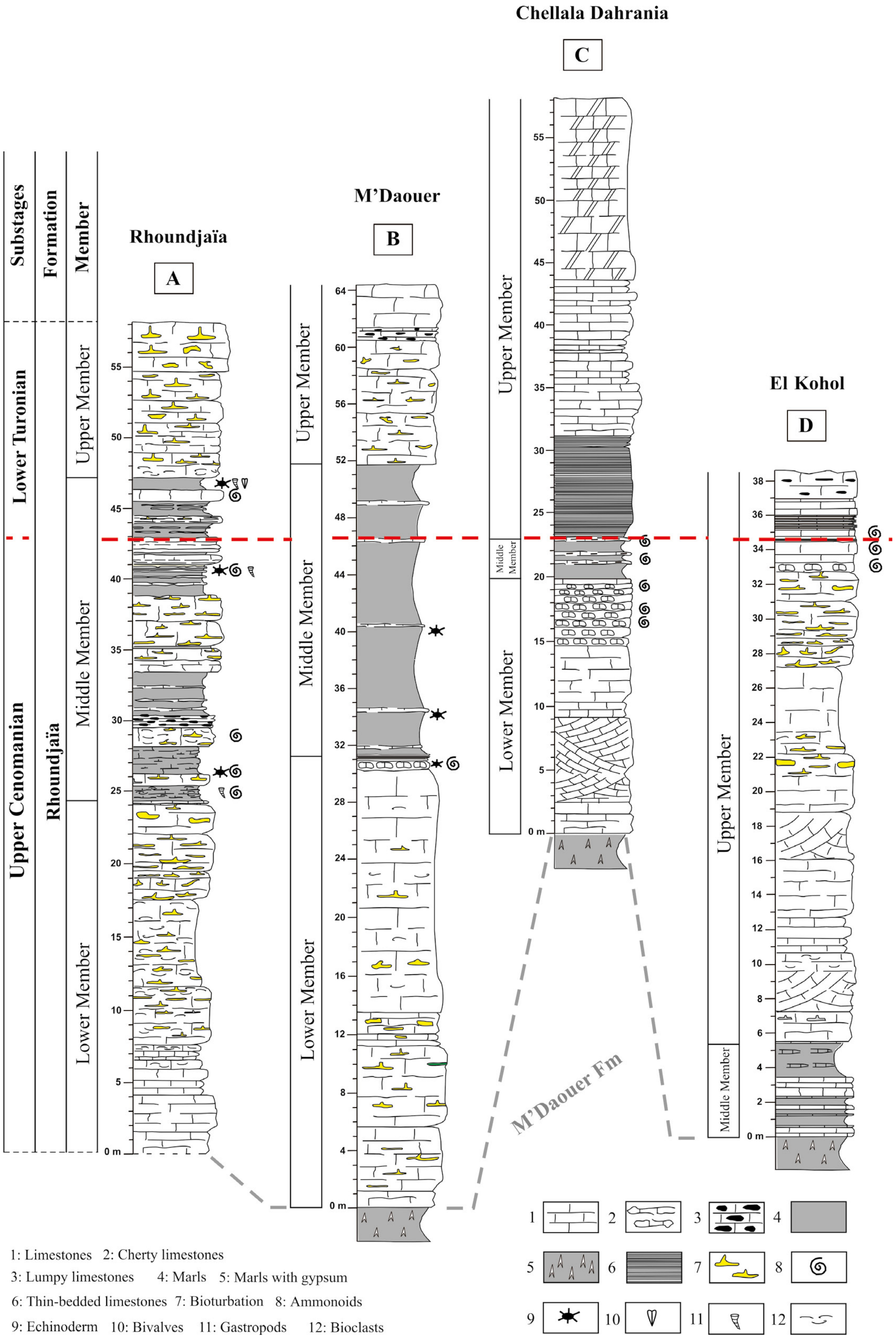

Figure 5.— Stratigraphic columns of the Rhoundjaïa, M'Daouer, Chellala Dahrania and El Kohol (A to D).

ments) and highly bioturbated limestone (*Thalassinoides*). Planktic foraminifera are scarce and only *Planoheterohelix moremani* is recorded.

In this section, the age of the Rhoundjaïa Formation is based on the palaeontological record. Thus, the few ammonites (*Vascoceras gamai* and *Vascoceras* sp.) collected in levels Rh-15', Rh-18', Rh-26' and Rh-29 indicate the upper Cenomanian. On the other hand, the ammonites collected in the bed Rh-31 and correlated with the M'Daouer sections give a lower Turonian age.

The last occurrence of *Rotalipora* at the top of bed Rh-5 would indicate the upper boundary of the *Rotalipora cushmani* Zone (Benadla *et al*., 2018). The beginning of the *Whiteinella archaeocretacea* Zone is signalled in the Rhoundjaïa section by the absence of *R. cushmani* and the record of *Helvetoglobotrunana praehelvetica* in bed Rh-6. According to the Robaszynski & Caron (1995) the base of the *W. archaeocretacea* Zone is defined by the last occurrence of *R. cushmani*. The record of *Helvetoglobotruncana praehelvetica* has been reported from the base of the *W. archaeocretacea* Zone (Wan *et al*., 2003).

M'Daouer section

This section was studied on the south-eastern flank of M'Daouer Mountain (Fig. 3B) (32º39'26.04"N, 0º04'46.15"W). With a thickness of 64.40 m, it is formed by two large limestone bars (Fig. 4B). This is the Rhoundjaïa Formation which shows the succession of three members (Fig. 5B):

- Lower Member (31.40 m) corresponds to massive beds of micritic and bioclastic limestone (wackestones to packstones of foraminifera, ostracods and filaments), affected by bioturbation (mainly *Thalassinoides*). At the top, this lower member ends in two lumpy beds (bioclastic wackestone rich in echinoderms and planktic foraminifera) very rich in echinoids and ammonites (*Vascoceras* sp., *V.* cf. *cauvini*, *V. gamai*, and *Neolobites vibrayeanus*) (Benadla, 2019). Planktic foraminifera are dominated by *Muricohedbergella planispira* and *M. delrioensis*, and *Planoheterohelix moremani* is exclusively recorded in the top of the member.
- Middle Member (20.20 m) is constituted mainly by marls with discontinuous beds of marly limestone (mudstones with filaments and planktic foraminifera) locally rich in irregular sea urchins (*Mecaster pseudofournelli*). *Planoheterohelix moremani*, *P. reussi*, *Guembelitria cenomana* and *G. cretacea* are very abundant whereas trochospiral forms such as *Muricohedbergella* are not recorded.
- Upper Member (12.80 m) comprises massive beds of bioturbated limestones followed by limestones with flint nodules and micritic limestone. Some beds are affected by dolomitization. The planktic foraminifera are scarce, dominated by small forms of *Planoheterohelix*, with secondary *Muricohedbergella*.

In the M'Daouer section, the ammonites collected (*Vascoceras* cf. *cauvini*, *V. gamai*, *Vascoceras* sp., and *Neolobites vibrayeanus*) and the foraminiferal record give to the Rhoundjaïa Formation an upper Cenomanian-lower Turonian age.

Chellala Dahrania section

Located in the eastern part of the Ksour Mountains, the Chellala Dahrania section was studied in the eastern end of the Milok El Guelbi Mountain (Fig. 3C) (33º05'32.27"N, 0º15'55.33"E). In this 58.40 m thick section (Fig. 4C), the Rhoundjaïa Formation consists of three members (Fig. 5C).

- Lower Member (19.60 m) overlies the gypsum-rich clays and silts of the M'Daouer Formation. It is formed mainly of micritic limestones (wackestones of planktic foraminifera), followed by channeled beds of slightly bioclastic limestones (wackestones to packstones with planktic and benthic foraminifera, and fragments of bivalves, gastropods and echinoderms) and micritic chalky limestones (mudstones to wackestones with planktic foraminifera). At the top, the member ends with a succession of decimetric beds of lumpy limestones with a nodular appearance, very rich in ammonites (*Vascoceras* cf. *gamai* and *Metoicoceras* aff. *geslinianum*). Planktic foraminifera in the lower part are mainly *Muricohedbergella planispira*, *M. delrioensis*, *Planispira moremani* and *P. reussi*, whereas to the top biserial (*Planoheterohelix*) and triserial forms (*Guembelitria*) are dominant.

- Middle Member (3.60 m) corresponds to an alternation of marly limestones and marls very rich in ammonites (*Vascoceras gamai* and *Vascoceras* sp.). Microfacies are wackestones rich in biserial and triserial planktic foraminifera.
- Upper Member (35.20 m) begins with a marly limestone bed with ammonites (*Choffaticeras* sp.), followed by a succession of micritic, slightly bioclastic limestones and massive dolomitic beds (mudstones to wackestones). Among the planktic foraminifera reappear the trochospiral form *Muricohedbergella*, but species of *Planoheterohelix* and *Guembelitria* keep dominant.

In this section the Rhoundjaïa Formation has provided an ammonite fauna (*Vascoceras gamai*, *Vascoceras* sp., *Choffaticeras* sp.) that indicate the upper Cenomanian-lower Turonian transition.

El Kohol section

The section was studied on the northern part of El Kohol Mountain (Fig. 3D) (33º03'17.03''N, 1º28'18.52''E). It is distinguished by the presence of a single bar marking the boundary between the M'Daouer and Rhoundjaïa formations (Fig. 4D). With a thickness of 38.65 m, in the Rhoundjaïa Formation can be recognised the upper two members (Fig. 5D):

- Middle Member (5.40 m) is resting concordantly on the gypsum-rich clays and silts of the M'Daouer Formation. It consists of alternating decimetric beds of bioclastic limestones (wackestones to packstones rich in fragments of echinoderms and bivalves) and marl, with discontinuous beds of micritic limestone (wackestones of bioclasts) at the top. *Thalassinoides* are locally common. Planktic foraminifera are not recorded.
- Upper Member (33.25 m) is constituted by micritic bioturbated limestones, sometimes in chanalised banks. The bioclastic limestones in pseudo-nodular beds are very rich in ammonites (*Vascoceras gamai* and *Vascoceras* sp.). This ensemble is followed by centimetric to decimetric beds of well-stratified limestones. These are essentially slightly bioclastic limestones (wackestones to packstones with echinoderms and foraminifera and locally rich in filaments) with ammonites (*Fikaites* sp.), platy limestones and flint nodules. Planktic foraminifera in the lower part (samples Kh-11 and Kh-12) are scarce and only represented by *Muricohedbergella planispira*. Biserial and triserial forms (*Planoheterohelix* and *Guembelitria*) appear and are abundant in the top of the member (from sample Kh-29 to Kh-44).

In the El Kohol section, the ammonites have enabled the two members of the Rhoundjaïa Formation to be dated with precision. Thus, the ammonites *Vascoceras gamai* with the foraminifera identified at the base give a upper Cenomanian age (*Muricohedbergella planispira*). Furthermore, the upper member of this formation has been dated to the lower Turonian thanks to the collection of a few ammonites of the genus *Fikaites*. It should be noted that Rerbal (2008) recorded in this member the ammonites *Pseudotissotia* sp. which confirms the lower Turonian.

Systematic palaeontology of ostracoda

The ostracod assemblages of the studied sections are characterised by the dominance of Family Cytherellidae (mainly genus *Cytherella*), followed by components of the families Paracyprididae (exclusively genus *Paracypris*) and Trachyleberididae (mainly genus *Cythereis*). Less common are components of families Bythocypridae and Macrocyprididae. The microfauna studied yielded 15 species, seven of which are left to open nomenclature. These taxonomic categories of ostracods belong to seven genera. In this systematics work, we adopted the classification of the European Register of Marine Species http://erms.biol.soton.ac.uk, and Integrated Taxonomic Information System http://www.itis.usda.gov. The systematic established by Horne *et al*. (2002) was also used to bring more precision to our work. Note that L, H, and W, represent measurements of length, height, and width respectively.

Class Ostracoda Latreille, 1802
Subclass Podocopa Sars, 1866
Order Platycopida Sars, 1866
Suborder Platycopina Sars, 1866
Superfamily Cytherelloidea Sars, 1866

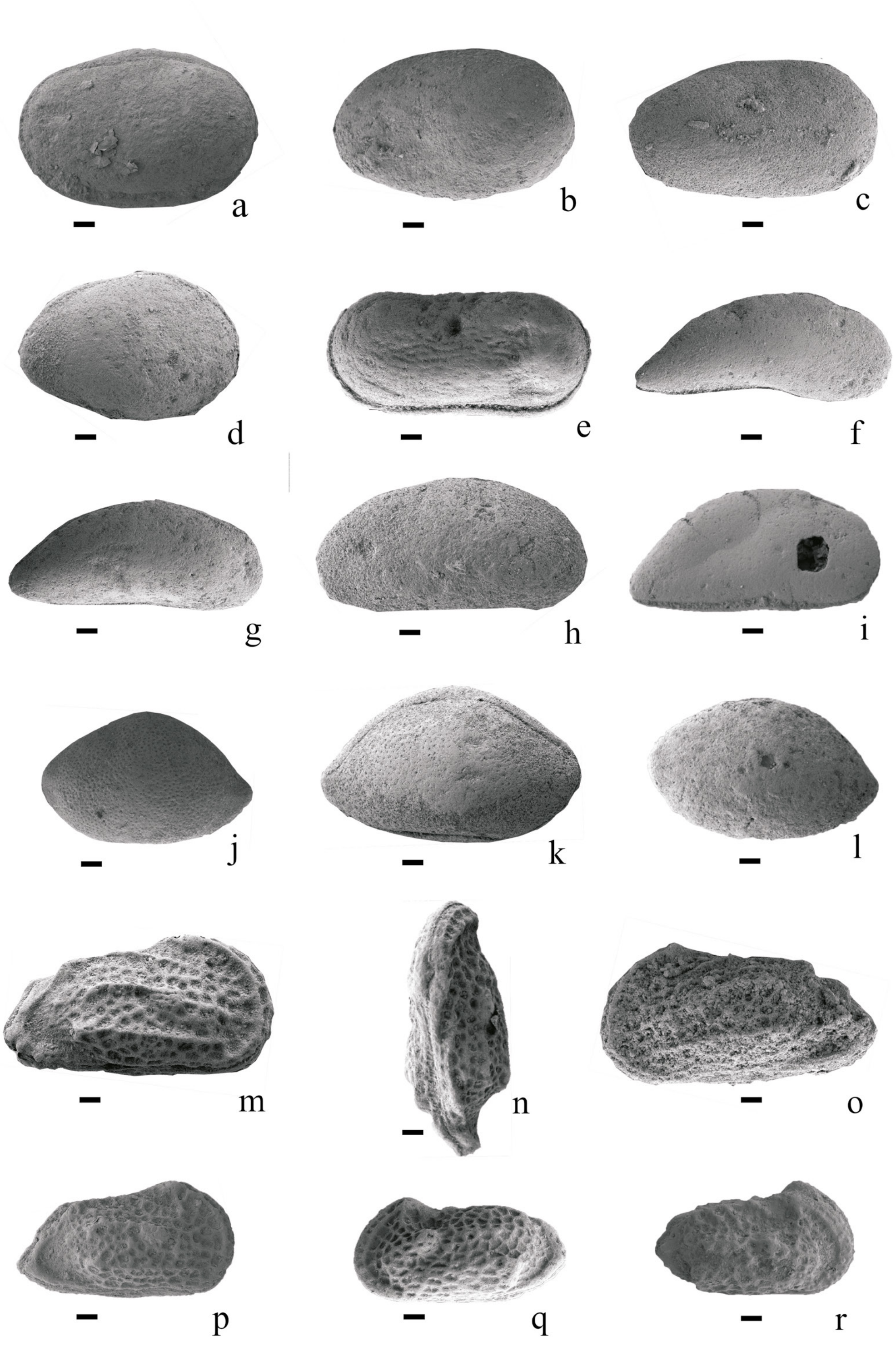

Figure 6.— Ostracods from the upper Cenomanian-lower Turonian (*Whiteinella archaeocretacea* Zone) of the Rhoundajaïa Formation. All are carapaces. Samples are indicated. a) *Cytherella* gr. *ovata,* left lateral view (Md-8_1); b) *Cytherella gigantosulcata*, right lateral view (Kh-3'); c) *Cytherella* sp. 1, left lateral view (Kh-3'); d) *Cytherella* ? sp. 2, left lateral view (Kh-3'); e) *Cytherelloidea* sp.*,* left lateral view (Rh-17'); f) *Paracypris dubertreti,* right lateral view (Md-8_3); g) *Paracypris mdaouerensis,*right lateral view (Md-8_3); h) *Bythocypris* sp., right lateral view (Kh-4'); i) *Macrocypris* sp., right lateral view (Rh-17'); j and k) *Bairdia* sp. 1, left lateral view (j), right lateral view (k) (Kh-4'); l) *Bairdia* sp. 2, left lateral view (Rh-17'); (m-o) *Cythereis mdaouerensis,* right lateral view (m), dorsal view (n), left lateral view (o) (Md-8_1)*;* p) *Cythereis ziregensis* right lateral view (Rh-17'); q) *Cythereis* sp. 1, left lateral view (Rh-31'); r) *Cythereis* sp. 2, right lateral view (Rh-31'). Scale bar = 50 µm.

Family Cytherellidae Sars, 1866
Genus *Cytherella* Jones, 1849
Cytherella gr. *ovata* Roemer, 1841
(Fig. 6a)

1841 *Cytherina ovata* Roemer, p. 104, pl. 16, fig. 21.
1845 *Cytherina ovata* Roemer; Reuss, p. 16, pl. 5, fig. 35.
1849 *Cythere* (*Cytherella*) *ovata* (Roemer); Jones, p. 28, pl. 7, figs. 24b-g.
1851 *Cytherina ovata* Roemer; Reuss, p. 48, pl. l 7, figs. 2b-d.
1899 *Cytherella obovata* (Roemer); Egger, p. 186, p l. 2 7, figs. 54-56.
1940 *Cytherella obovata* (Roemer); Bonnema, p. 93, pl. l , figs. 1- 1 6.
1952 *Cytherella obovata* (Roemer); Dupper, p. 106, pl. 5 , fig. 3.
1956 *Cytherella obovata* (Roemer); Deroo, p. 1508, pl. l, fig s. 4-6.
1966 *Cytherella obovata* (Roemer); Gründel, p. 12, pl. 1, fig. 2.
1969 *Cytherella* gr. *ovata* Roemer; Bassoullet & Damotte, pl. 2, fig. 13.
1974 *Cytherella ovata* Roemer; Damotte & Freytet, p. 207, pl. I, fig. 1.
1976 *Cytherella* "*ovata*" (Roemer); Bremen, p. 82, pl. l , fig . la-b.
1980 *Cytherella* gr. *ovata* Roemer; Babinot, pl. 1, figs. 12, 13; pl. 2, figs. 1-3.
1991 *Cytherella* gr. *ovata* Roemer; Shahin, p. 133, pl. 1, fig. 5.
2006 *Cytherella* aff. *ovata* Roemer; Andreu & Bilotte, p. 59, pl. 1, figs. 1-5.
2008 *Cytherella ovata* Roemer; El-Nady *et al*., p. 561, pl. I, fig. 6.
2018 *Cytherella* gr. *ovata* Roemer; Benadla *et al.,* p. 420, figs. 8A-C.

Material: More than 200 specimens.

Dimensions: L: 0.08–0.62 mm; H: 0.06–0.40 mm; W: 0.02–0.28 mm.

Locality: Rhoundjaïa, M'Daouer, Chellala Dahrania and El Kohol.

Description: Form of genus *Cytherella*, ovoidal to subquadrangular in lateral view. The species is charaterized by an oval outline. Right valve larger, overlapping left valve along entire periphery. Posterior and anterior margin are rounded. Valve surface is smooth.

Age: Upper Cenomanian-lower Turonian.

Stratigraphic and geographic distribution: *Cytherella* gr. *ovata* is known from the lower Cenomanian of Egypt (El-Nady *et al*., 2008), upper Cenomanian-Turonian of the Western Saharan Atlas (Bassoullet & Damotte, 1969) and Tinrhert Basin of eastern Algeria (Tchenar *et al*., 2020), France (Babinot, 1980; Jolet *et al*., 2001; Andreu & Bilotte, 2006) and Egypt (Shahin, 1991; Shahin *et al*., 1994). It has also been identified in the Turonian-Coniacian of the Tunisian Atlas (Salmouna *et al*., 2014) and in general, the Upper Cretaceous of Europe and America (Damotte & Freytet, 1974).

Cytherella gigantosulcata Rosenfeld, 1974
(Fig. 6b)

1932 *Cytherella sulcata* Van Veen, p. 336, pl. 4, figs. 1-18
1959 Ostracode U. 10 Glintzboeckel & Magne, p. 64, pl. 3, fig. 31
1969 *Cytherella ?* U. 10 Glintzboeckel & Magne; GREKOFF, pl. 1, fig. 6
1977 *Cytherella sulcata* Rosenfeld; Al Abdul Razzaq, p. 50, pl. 4, figs. 1-5
1980 *Cytherella sulcata* Rosenfeld; Ben Youssef, p. 92, pl. 5, figs. 6-8
1981 *Cytherella sulcata* Rosenfeld; Bismuth *et al*., p. 223, pl. 6, figs. 3-4
1983 *Cytherella sulcata* Rosenfeld; Gargouri & Razgallah, p. 148, pl. 33. fig. 1
1988 *Cytherella posterosulcata* Rosenfeld; Athersuch, p. 202, pl. 5, fig. 1.
1991 *Cytherella gigantosulcata* Rosenfeld; Szczechura *et al*., pl. 1, figs. 7-12.
2008 *Cytherella sulcata* Rosenfeld; El-Nady *et al*., p. 561, pl. I, fig. 13.
2013 *Cytherella gigantosulcata* Rosenfeld; Shahin & Elbaz, p. 107, pl. 1, figs. 9-10.
2016 *Cytherella gigantosulcata* Rosenfeld; Bergue *et al*., p. 199, fig. 2 f-g.
2022 *Cytherella gigantosulcata* Rosenfeld; Slami *et al*., p. 9, figs. 4.1-4.5.

Material: 11 specimens.

Dimensions: L: 0.88 mm; H: 0.55 mm; W: 0.44 mm.

Locality: El Kohol.

Description: Carapace of medium size, oval in lateral view. Anterior margin is rounded and slightly compressed in dorsal view. Posterior margin is strongly rounded and larger. Dorsal and ventral margins are curved. Maximum height at mid-length. Valve surface is smooth.

Age: Upper Cenomanian

Stratigraphic and geographic distribution: This species has been collected in the Cenomanian of Tunisia (Glintzboeckel & Magné, 1959; Grekoff, 1969; Bismuth *et al*., 1981), Tinrhert Basin of eastern Algeria (Tchenar *et al*., 2020), Morocco (Andreu, 1989), Iran (Grosdidier, 1973), Kuwait (Al-Abdul-Razzaq, 1979) and Egypt (Hataba & Ammar, 1990; Shahin, 1991; El-Nady, 2008). In Jordan, it has been collected from the upper Cenomanian (Babinot & Basha, 1985) and the upper Albian-lower Cenomanian (Bergue *et al*., 2016).

Cytherella sp.1 Ruault-Djerrab, 2012
(Fig. 6c)

2012 *Cytherella* sp.1 Ruault-Djerrab, p. 195, pl. 3, fig. F.
2013 *Cytherella* sp.1 Andreu *et al.*, p. 237, pl. 1, figs. 1-4.
2018 *Cytherella* sp.1 Benadla *et al.*, p. 420, fig. 8D-E.

Material: More than 200 specimens.
Dimensions: L: 0.13-0.73 mm; H: 0.06-0.42 mm; W: 0.04-0.26 mm.
Locality: Rhoundjaïa, M'Daouer, Chellala Dahrania and El Kohol.
Description: Medium-size carapace, valves are elongated and subequal. The right valve is slightly larger than the left valve with an almost identical outline. Dorsal margin straight. Ventral margin becoming concave postero-dorsally. Posterior and anterior margins simmetrically rounded.
Age: Upper Cenomanian-lower Turonian.
Stratigraphic and geographic distribution: Middle to Upper Cretaceous of southeast Constantine, Algeria (Ruault-Djerrab, 2012) and the upper Cenomanian-lower Turonian of Morocco (Andreu *et al*., 2013).

Cytherella ? sp. 2 Ruault-Djerrab, 2012
(Fig. 6d)

Material: More than 200 specimens.
Dimensions: L: 0.08–0.55 mm; H: 0.11–0.35 mm; W: 0.06-0.22 mm.
Description: Form potentially assigned to genus *Cytherella.* Oval in lateral view. Dorsal and ventral margins have very strong ray of curvature. Maximum height at mid-length. The right valve overlaps the left valve along the entire periphery. In dorsal or ventral view, the outline lozenge, subrombic is very characteristic, regular and rounded.
Locality: Rhoundjaïa and M'Daouer.
Age: Upper Cenomanian-lower Turonian.
Stratigraphic and geographic distribution: The Cenomanian-Coniacian of the South-East Constantine, Algeria (Ruault-Djerrab, 2012) and the Maastrichtian of the El Koubbat syncline of the Middle Atlas of Morocco (Andreu & Tronchetti, 1996).

Genus *Cytherelloidea* Alexander, 1929
Cytherelloidea sp.
(Fig. 6e)

Material: Seven specimens.
Dimensions: L: 0.42–0.57 mm; H: 0.28 mm; W: 0.11-0.15 mm.
Locality: Rhoundjaïa, M'Daouer and El Kohol
Description: Subrectangular in lateral view, sculpted (nets ornamentation, muri and reticules). Anterior and posterior margins are well rounded. Dorsal and ventral margins concave at mid-length. Ribs are longitudinal, short and sinuous.
Age: Upper Cenomanian-lower Turonian.

Suborder Podocopina Sars, 1866
Superfamily Cypridoidea Baird, 1845
Family Paracyprididae Sars, 1923
Genus *Paracypris* Sars, 1866
Paracypris dubertreti Damotte and Saint-Marc, 1972
(Fig. 6f)

1972 *Paracypris dubertreti* Damotte & Saint-Marc, Pl. I, fig. 6.
1972 *Paracypris dubertreti* n. sp. Damotte & Saint-Marc, p. 276, pl. 1, fig. 1.
1974 *Paracypris acutocaudata* n. sp. Rosenfeld, p. 8, pl.1, figs. 22-24.
1977 *Paracypris* sp. 1 Al Abdul Razzaq, p. 87, pl. 15, figs. 1-3.
1985 *Paracypris dubertreti* Damotte & Saint-Marc; Viviere, p.149, pl. 3, figs. 6–7
1994 *Paracypris acutocaudata* Rosenfeld; Shahin *et al.,* p. 41, pl. 1, fig. 23.
1999 *Paracypris acutocaudata* Rosenfeld; Ismail, p. 310, pl. 3, figs. 16–17.
2001 *Paracypris dubertreti* Damotte & Saint-Marc; Hewaidy & Morsi, p. 239, pl. 2, fig. 6.
2008 *Paracypris acutocaudata* Rosenfeld; El-Nady *et al*., p. 563, pl. II, figs. 11-12.
2013 *Paracypris dubertreti* Damotte & Saint-Marc; Shahin & Elbaz, p. 107, pl. 1, fig. 30.
2016 *Paracypris dubertreti* Damotte & Saint-Marc; Bergue *et al*., p. 201, figs. 3K-L.
2018 *Paracypris dubertreti* Damotte & Saint-Marc; Benadla *et al*., p. 201, p. 420, fig. 8F.

Material: More than 200 specimens.
Dimensions: L: 0.33-0.68, H: 0.15-0.33 mm, W: 0.06-0.22 mm.

Locality: Rhoundjaïa, M'Daouer, Chellala Dahrania and El Kohol.

Description: This species is characterised by posterior margin very tapering and pointed. Anterior margin well rounded. Valve surface smooth and becoming strongly arched ventrally. Dorsal margin straight at mid-length.

Age: Upper Cenomanian-lower Turonian.

Stratigraphic and geographic distribution: This species has been described in the Aptian-Cenomanian of Egypt (Boukhary *et al*., 1977; Shahin *et al*., 1994; Ismail, 1999; Morsi & Bauer, 2001; Hewaidy & Morsi, 2001; Bassiouni, 2002), middle and upper Cenomanian of Lebanon (Damotte & Saint-Marc, 1972) and Jordan (Morsi & Wendler, 2010), Cenomanian-Turonian of Algeria (Vivière, 1985; Majoran, 1989; Slami *et al*., 2022), middle Cenomanian of Morocco (Andreu, 1991), middle Cenomanian-lower Turonian of central Egypt (Boukhary *et al*., 2009; Shahin & Elbaz, 2013a, b), lower Turonian of South-East Constantine Algeria (Ruault-Djerrab, 2012), Turonian of the Potiguar Basin, North-East Brazil (Poivesan *et al*., 2014) and finally the Turonian-Coniacian of the Tunisian Atlas (Salmouna *et al*., 2014).

Paracypris mdaouerensis Bassoullet & Damotte, 1969
(Fig. 6g)

1969 *Paracypris mdaouerensis* n. sp. Bassoullet & Damotte, p. 143, pl. 2, fig. 10.
1996 *Paracypris* cf. *mdaouerensis* Bassoullet & Damotte; Andreu & Tronchetti, p.57, pl. 5, figs. 18-19
2000 *Paracypris* aff. *mdaouerensis* Bassoullet & Damotte; Viviers *et al*., p. 418, fig. 10, n°12, 13, 16.
2001 *Paracypris mdaouerensis* Bassoullet & Damotte; Morsi & Bauer, p. 386, pl. 2, fig. 6.
2008 *Paracypris mdaouerensis* Bassoullet & Damotte; El-Nady *et al*., p. 563, pl. II, fig. 13.
2012 *Paracypris mdaouerensis* Bassoullet & Damotte; Ruault-Djerrab, p. 195, pl. 3, fig. A., pl. 10, fig. A.
2013 *Paracypris mdaouerensis* Bassoullet & Damotte; Shahin & Elbaz, p. 107, pl. 1, figs. 31-32.
2018 *Paracypris mdaouerensis* Bassoullet & Damotte; Benadla *et al*., p. 420, figs. 8G-H.
2022 *Paracypris mdaouerensis* Bassoullet & Damotte; Slami *et al*., p. 12, figs. 7.1-7.2.

Material: More than 200 specimens.

Dimensions: L: 0.17–0.8 mm; H: 0.06–0.33 mm; W: 0.04–0.22 mm.

Locality: Rhoundjaïa, M'Daouer and Chellala Dahrania

Description: Similar to *Paracypris dubertreti*, but it differs in its ventral margin which is not arched.

Age: Upper Cenomanian-lower Turonian.

Stratigraphic and geographic distribution: The species *Paracypris mdaouerensis* collected for the first time in the Monts des Ksour (Bassoullet & Damotte, 1969) has been cited in the lower Cenomanian of Jordan (Babinot & Basha, 1985), the Cenomanian of Gabon (Neufville, 1973), the Albian-Cenomanian of the Brazilian Basin (Viviers *et al*., 2000), the Cenomanian to Coniacian-Santonian of the Eastern Saharan Atlas of Algeria (Ruault-Djerrab, 2012; Mebarki *et al*., 2016; Slami *et al*., 2022), and Tinrhert Basin of eastern Algeria (Tchenar *et al*., 2020), the lower Cenomanian-Turonian of Egypt (El-Nady *et al*., 2008; Shahin & Elbaz, 2013a, b) and Morocco (Andreu, 1989; Ettachfini *et al*., 2005), in the Turonian-Coniacian of the Tunisian Atlas (Salmouna *et al*., 2014) and the Albian-Turonian of Morocco (Andreu, 1991; Andreu & Tronchetti, 1996; Andreu *et al*., 2013).

Family Bythocyprididae Maddocks, 1969
Genus *Bythocypris* Brady, 1880
Bythocypris sp.
(Fig. 6h)

Material: 50 specimens.

Dimensions: L: 0.26–0.77 mm; H: 0.28 mm; W: 0.06-0.15 mm.

Locality: Rhoundjaïa, M'Daouer, Chellala Dahrania and El Kohol.

Description: Carapace of medium size. Subrectangular to suboval in lateral view, tighten and convex in dorsal view. Maximum height at mid-length. The left valve overlaps the right valve along the entire periphery, except the dorsal view. Ventral margin straight. Valve surface smooth.

Age: Upper Cenomanian-lower Turonian.

Family Macrocyprididae Müller, 1912
Genus *Macrocypris* Brady, 1867
Macrocypris sp.
(Fig. 6i)

Material: 20 specimens.
Dimensions: L: 0.48–0.73 mm; H: 0.40–0.42 mm; W: 0.11-0.22 mm.
Locality: Rhoundjaïa, M'Daouer, Chellala Dahrania and El Kohol.
Description: Studied carapace are usually deformed. Anterior margin truncated and extends downwards. The right valve overlaps the left valve along the entire periphery. Dorsal margin sinuous along anterior margin**.**
Age: Upper Cenomanian-lower Turonian.

Superfamily Bairdioidea Sars, 1865
Family Bairdiidae Sars, 1885
Genus *Bairdia* McCoy, 1844
Bairdia sp.1
(Fig. 6j, k)

Material: 50 specimens.
Dimensions: L: 0.80-1.11 mm; H: 0.46–0.73 mm; W: 0.31-0.37 mm.
Locality: Rhoundjaïa and El Kohol.
Description: Carapace of large size, smooth and finely porous. Anterior margin short, pointed and slightly turned up. Posterior margin tapered and rounded. Dorsal margin strongly convex with inflection well marked in the two extremity. Ventral margin convex to subrectlinear in mid-length. The left valve overlaps the right valve along the entire periphery.
Age: Upper Cenomanian.

Bairdia sp. 2
(Fig. 6l)

Material: 22 specimens.
Dimensions: L: 0.84-1.11 mm; H: 0,53-0,64 mm; W: 0.31-0.48 mm.
Locality: Rhoundjaïa, M'Daouer and El Kohol.
Description: Carapace elongated and smooth. Dorsal margin convex with sharp inflection at extremity. Ventral margin convex. Anterior margin rounded. Posterior margin short and pointed. The left valve overlaps right valve along the entire periphery.
Age: Upper Cenomanian.

Superfamily Cytheroidea Baird, 1850
Family Trachyleberididae Sylvester-Bradley, 1948

Genus *Cythereis* Jones, 1849
Cythereis mdaouerensis Bassoullet & Damotte, 1969
(Fig. 6m, n, o)

1969 *Cythereis mdaouerensis* n. sp. Bassoullet & Damotte, p. 141, pl. 1, fig. 5.
2018 *Cythereis mdaouerensis* Bassoullet & Damotte; Benadla *et al*., p. 420, fig. 8M-O.

Material: More than 100 specimens.
Dimensions: L: 0.11-0.64 mm; H: 0.06–0.33 mm; W: 0.03–0.26 mm.
Locality: Rhoundjaïa, M'Daouer and Chellala Dahrania.
Description: Rectangular shape in lateral view, ornament with a network reticulations. Anterior margin rounded in a semicircle. Posterior margin pointed. We note the presence of three fine longitudinal ribs. Median ribs prolong to subcentral tubercle in continuity. Ventral ribs are located clearly above the ventral margin that it does not cover.
Age: Upper Cenomanian-lower Turonian.
Stratigraphic and geographic distribution: The upper Cenomanian-lower Turonian of the Western Saharan Atlas (Bassoullet & Damotte, 1969; Bassoullet, 1973) and the lower Turonian of Tunisia (Bismuth *et al*., 1981).

Cythereis ziregensis Bassoullet & Damotte, 1969
(Fig. 6p)

?1959 Ostracode E8 Glintzboeckel & Magné, pl. 3, fig. 32.

Material: 20 specimens.
Dimensions: L: 0.46-0.66 mm; H: 0.28-0.31 mm; W: 0.26 mm.
Locality: Rhoundjaïa and M'Daouer.
Description: Subrectangular in lateral view, flattened laterally in dorsal view. Dorsal margin straight, very long, underlined by a denticulate ridge on its outer edge. Ventral margin short, slightly inclined and up towards the posterior margin. Anterior margin rounded almost in a semicircle. Posterior margin triangular, denticulate. Median ribs is non-existent. Low convexity forms the subcentral tubercle.
Age: Upper Cenomanian.
Stratigraphic and geographic distribution: Upper Cenomanian of the Western Saharan Atlas (Bassoullet & Damotte, 1969).

Cythereis sp. 1
(Fig. 6q)

Material: 11 specimens.
Dimensions: L: 0.69 mm; H: 0.38 mm; W: 0.22 mm.
Locality: Rhoundjaïa, El Kohol and Chellala Dahrania.
Description: The specimens differ from other individuals of *Cythereis* by the presence of cross-linking along the entire surface and the lateral costulation fading slightly in the mid-lenght of the valve.
Age: Upper Cenomanian.

Cythereis sp. 2
(Fig. 6r)

Material: 5 specimens.
Dimensions: L: 0.65 mm; H: 0.35 mm; W: 0.23 mm.
Locality: Rhoundjaïa.
Description: Specimens shows deterioration of ornamentation which results in the appearance of irregular tubers at the posterior endings of ventral and dorsal ribs, as well as in the mid-length of the carapace.
Age: Upper Cenomanian.

Interpretation and comparison with other regions

The ostracod fauna of the upper Cenomanian-lower Turonian transition in the Ksour and Amour mountains has been previously studied and figured by Bassoullet & Damotte (1969) and Benadla (2019) in which several species determined for the first time, remain endemic. From a biostratigraphic point of view, two assemblages of ostracods could be found in the Cenomanian-Turonian transition (Figs 7-10).

- The first rich and diverse assemblage consists of *Cytherella* gr. *ovata*, *Cytherella gigantosulcata, Cytherella* sp. 1, *Cytherelloidea* sp., *Paracypris dubertreti*, *Paracypris mdaouerensis*, *Bythocypris* sp., *Macrocypris* sp., *Bairdia* sp. 1, *Bairdia* sp. 2, *Cythereis ziregensis*, *Cythereis mdaouerensis*, *Cythereis* sp. 1, and *Cythereis* sp. 2. This species assemblage indicates an upper Cenomanian age. At the North Africa scale, this recognised association in the Western Saharan Atlas corresponds to *Cythereis algeriana* Zone defined in Tunisia (Bismuth *et al*., 1981) and in Egypt (Ismail, 2001).
- The second assemblage, which is very rich but not very diverse, consists mainly of *Cytherell*a sp. 2, and *Cytherelloidea* sp., and secondarily by *Cytherella* gr. *ovata*, *Cythereis mdaouerensis*, *Paracypris dubertreti*, *Paracypris mdaouerensis*, *Cytherell*a sp. 1, This association indicates a lower Turonian age and corresponds to *Cythereis mdaouerensis* Zone (Bismuth *et al*., 1981).

The ostracod assemblages determined for the stratigraphic interval of the Cenomanian-Turonian transition indicate the presence of a biological event corresponding to the explosion of smooth ostracods called the Cytherellid Event, also described in Spain (Barroso-Barcenilla *et al*., 2011), Egypt (Shahin & Elbaz, 2013a) and Algeria (Benadla *et al*., 2018). Cytherellids are relatively resistant to oxygen depleted conditions (Whatley, 1991, 1995) and *Cytherella* has been interpreted as an ostracod indicative of warm waters adapted to survive during low oxygen episodes (Depêche, 1984; Whatley, 1995; Bonnet *et al*., 1999; N'Zaba-Makaya *et al*., 2003; Reolid, 2020; Reolid & Ainsworth, 2022). In the Rhoundjala section the Cytherellid Event coincides with the negative carbon isotopic excursion of the OAE2 (Benadla *et al*., 2018).

Intra-family comparisons with other regions

This analysis compare the ostracod assemblages from Moroccan Basin (MB; Agadir Basin, Central High Atlas Basin, Middle Atlas Basin), Algerian Basin (AB; Ksour Sub-basin, Amour Sub-basin, Tébessa Sub-basin), Central Tunisian Basin (TB), Egyptian Basin (EB, East and Central Sinai Basin), Lebanese Basin (LB), Central Jordanian Basin (JB), and Western Oman Basin (OB).

The results of the processing of the generic matrix by the program *PAST*-Palaeontological *STatistics*, ver.1.89 (Hammer *et al*., 2009; Table 1) are presented in the form of planar graphs (principal coordinate analysis, PCA) (Fig. 11A) and trees whose branch lengths are proportional to the distance between the taxonomic composition of the different regions (Fig. 11B). Thus, the intra-family generic diversity shows the following structure:

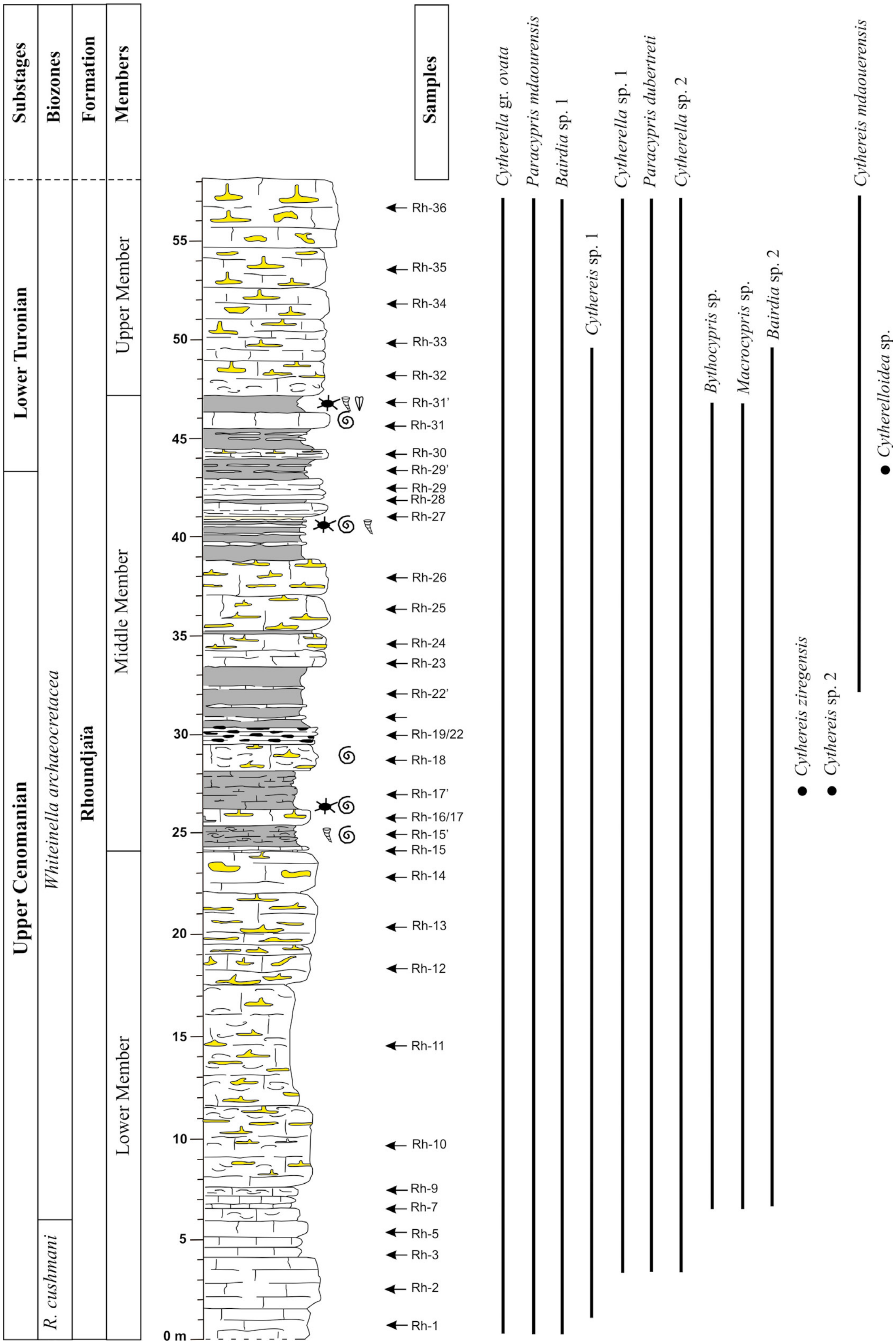

Figure 7.— Stratigraphic distribution of species of ostracods recorded in Rhoundjaïa section.

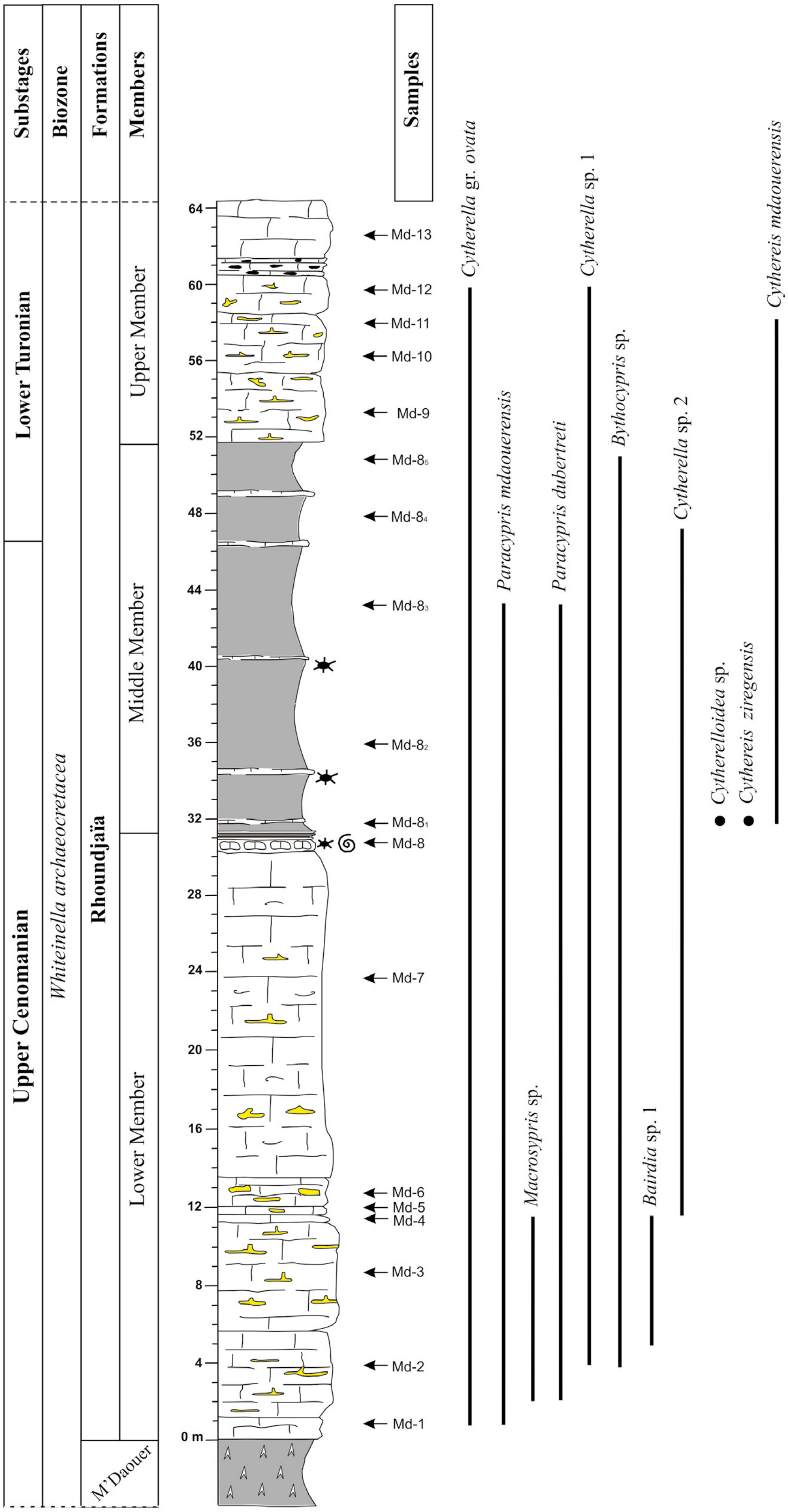

Figure 8.— Stratigraphic distribution of species of ostracods recorded in M'Daouer section.

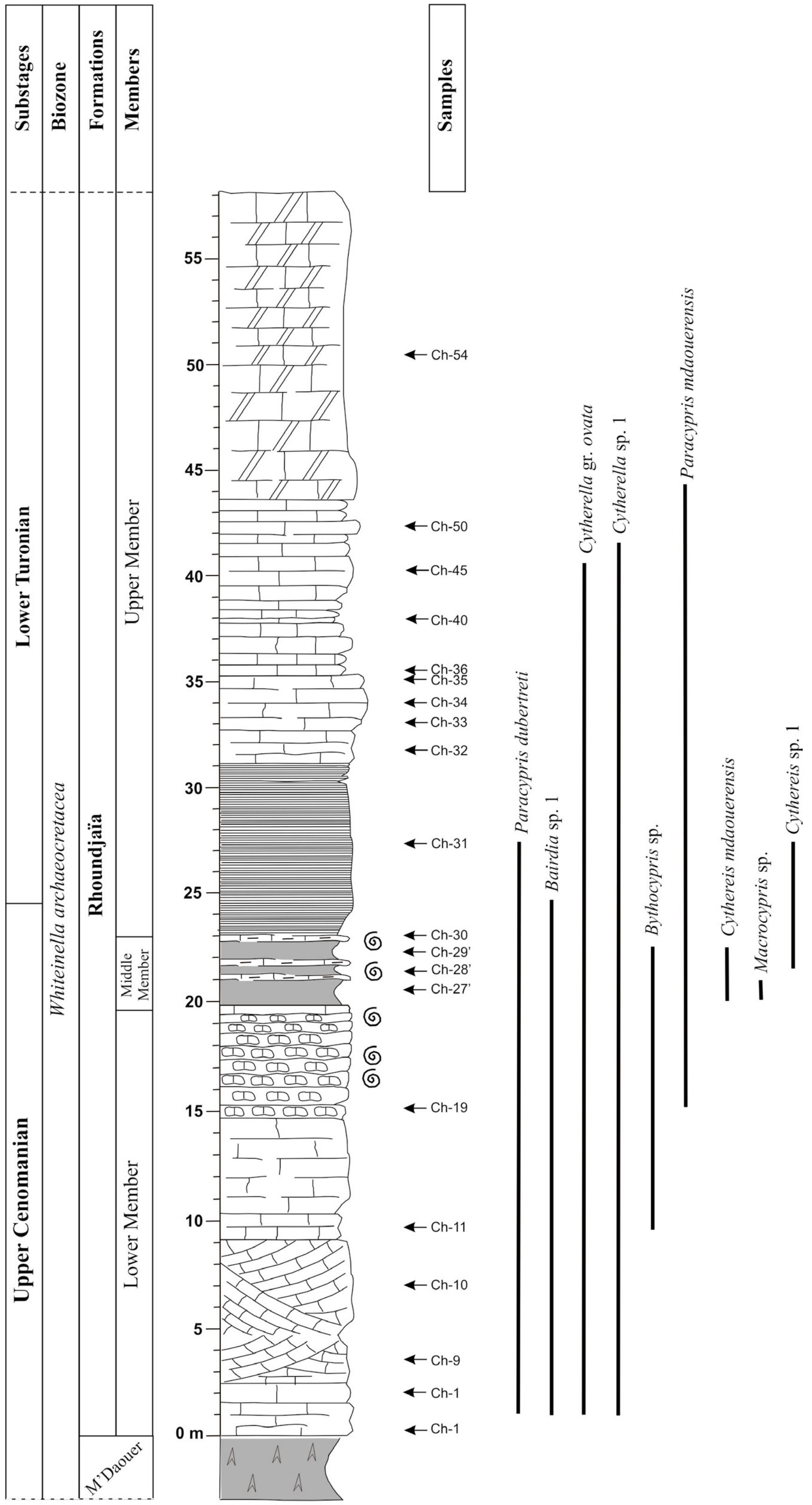

Figure 9.— Stratigraphic distribution of species of ostracods recorded in Chellala Dahrania section.

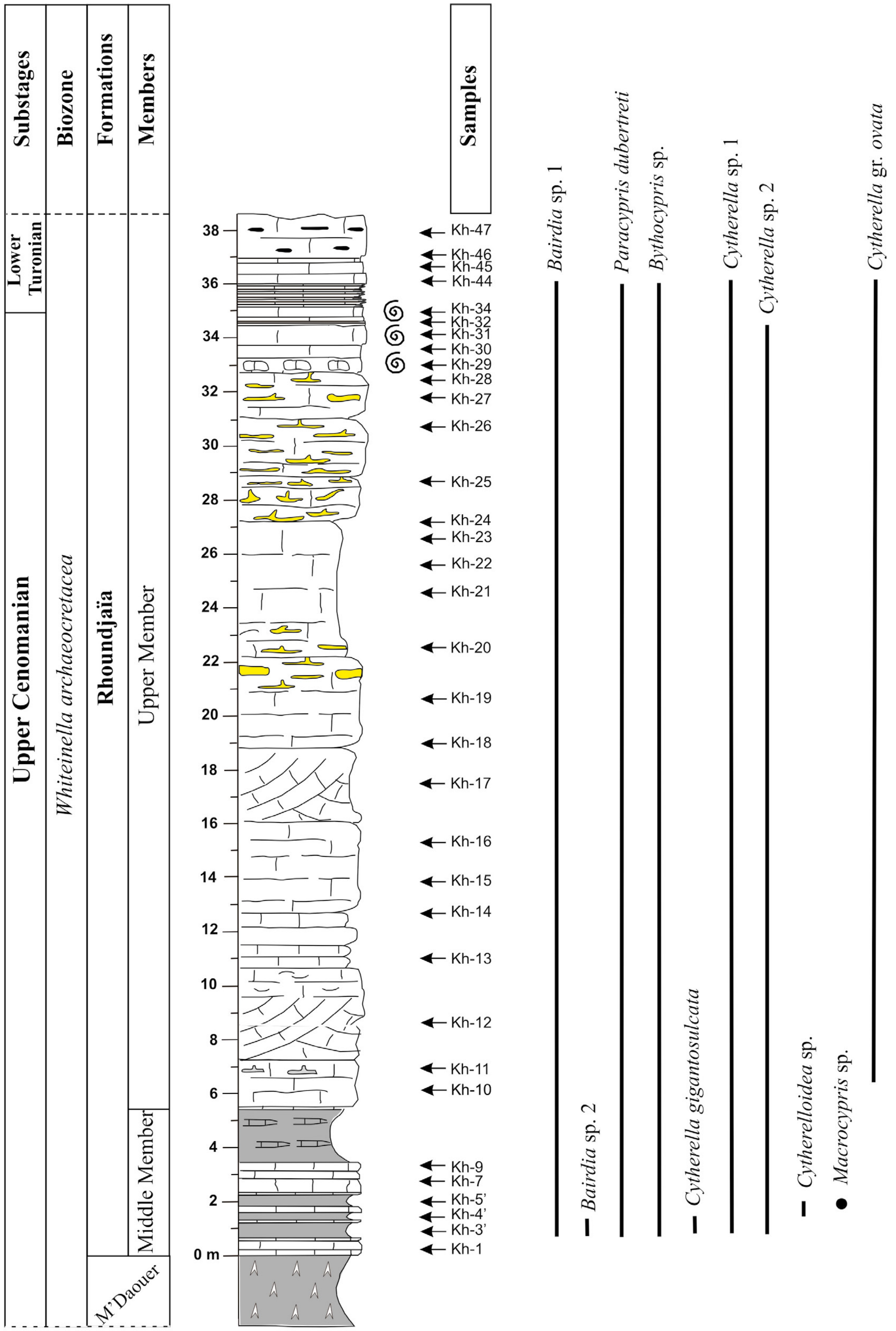

Figure 10.— Stratigraphic distribution of species of ostracods recorded in El Kohol section.

a) A first group made up of assemblages from basins belonging to four regions: Morocco (MB), Egypt (EB), Jordan (JB) and Oman (OB), which are more or less isolated on figures 11A, B.
b) A second group formed by the Algerian Saharan Atlas basins (AB) and Central Tunisian Basin (TB). It should be noted that the generic intra-family composition of the study region (Ksour and Amour mountains) is relatively close to Jordanian Basin.
c) Finally, the Central Lebanese Basin (LB) is isolated.

These different basins on the northern edge of Gondwana show an abundance of smooth forms represented by families Cytherellidae, Cytherideidae, Cytheruridae and Paracyprididae, and usually ornamented individuals of Trachyleberidae. In the Saharan Atlas Basin Cytherellidae and Paracypridae dominated during the Cenomanian-Turonian transition.

Previous works by Khalil (2020) and Shahin & Elbaz (2021) have stablished two different bioprovinces for Ostracoda: the North African Province (or South Tethysian Province; Shahin & Elbaz, 2021) including Morocco, Algeria, Tunisia and Egypt, and the Middle East Province including Lebanon, Oman, Saudi Arabia, Kuwait and Iran. Mebarki *et al*. (2016) found that ostracod species from Guir Basin (southwestern part of Saharan Atlas) are closer in affinity to those from Atlasic Basin of Morocco, and secondarily with assemblages fropm Tunisia and Egypt. Our results differ from these other proposals but have in common the dominance of smooth ostracods, mainly cytherellids, during the Cenomanian-Turonian transition.

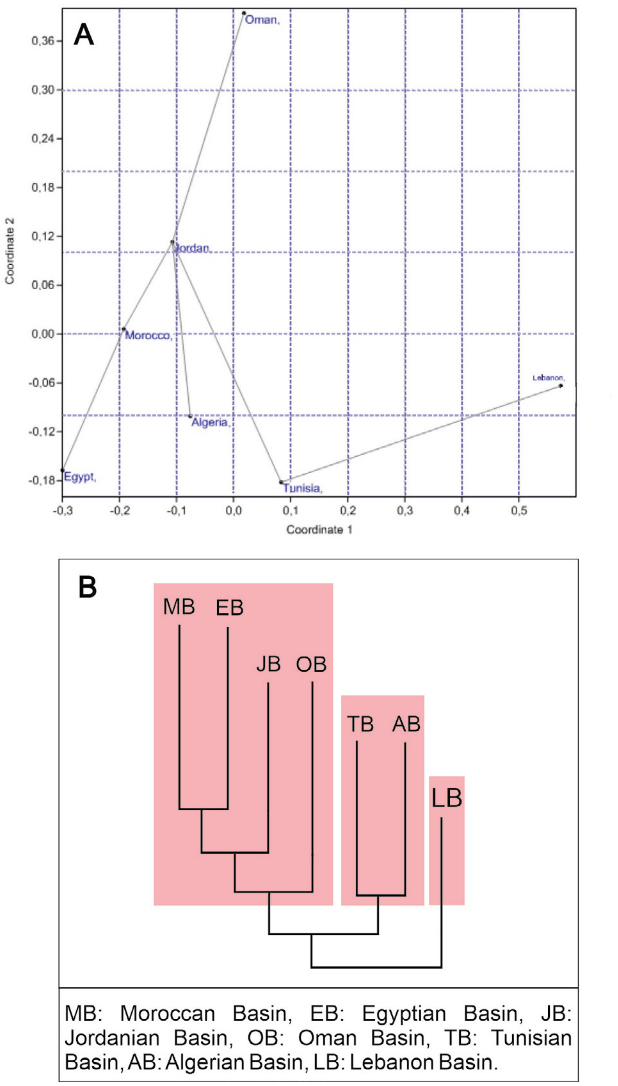

Figure 11.— A. Principal coordinates analysis (PCA) of the distance matrix of Bray-Curtis. B. Phenogram (tree of Neighbor-Joining) allowing the visualization of the proximity between basins as recorded in the distance matrix of Bray-Curtis.

Quantitative comparison of the taxonomic composition with other regions

In this biogeographical quantification analysis, we dealt with 48 genera of which 33 (68%) are present in the Egyptian basins. The results given in the form of a phenogram (Fig. 12A) and a hierarchical association diagram (Fig. 12B), allowed us to reconstitute the following topology:

a) Proximity of the ostracod fauna of the Moroccan and Egyptian basins. These two regions share 12 genera (25%) (*Bairdia*, *Brachycythere*, *Cythereis*, *Cytherella*, *Limburgina*, *Metacytheropteron*, *Nigeroloxoconcha*, *Ovocytheridea*, *Parakrithe*, *Paracypris*, *Reticulocosta*, and *Spinoleberis*). To the Moroccan and Egyptian basins, the two basins belonging to the Middle East, Jordanian and Oman basins, are related, the Central Jordanian Basin with 4 genera in common (*Brachycythere*, *Cythereis*, *Cytherella*, and *Parakrithe*) and the Oman Basin with 4 genera in common (*Brachycythere*, *Cythereis*, *Cytherella*, and *Metacytheropteron*).

b) The ostracod fauna of the Algerian and Tunisian basins are very similar. This resemblance is reflected in the presence of 5 shared genera to both regions (*Cythereis*, *Cytherella*, *Cytheropteron*, *Dolocytheridea*, and *Paracypris*).
c) The remoteness of the ostracod fauna of Lebanese Basin compared to the regions analysed.

The similarity between the ostracod faunas from different basins shows the probable existence of communication routes during the Cenomanian-Turonian transition or the existence of equivalent palaeoenvironmental conditions.

Pielou criteria Test

The obtained values of Q/Qmax (Table 2) show that the matrix, MB (Morocco), AB (Algeria), TB (Tunisia), EB (Egypt), LB (Lebanon), JB (Jordan), OB (Oman) is completely disordered (ungraded matrix). The order of the list of regions does not follow any geographical sequence.

Conclusions

The study of ostracods from the Cenomanian-Turonian transition (*Whiteinella archaeocretacea* Zone) through four sections surveyed in the Ksour Mountains (Western Saharan Atlas) and the Amour Mountains (Central Saharan Atlas) allowed the identification of fifteen species, seven genera and five families. The average ostracod assemblage is dominated by the Family Cytherellidae (mainly genus *Cytherella*), and secondarily by the families Paracyprididae (exclusively *Paracypris*) and Trachyleberididae (mainly *Cythereis*). Less common are components of families Bairdiidae, Bythocypridae and Macrocyprididae.

Two ostracod biozones have been identified within the *Whiteinella archaeocretacea* foraminiferal Zone, the *Cythereis algeriana* Zone of the upper Cenomanian, and the *Cythereis mdaouerensis* Zone of the lower Turonian.

From palaeoecological point of view, the studied assemblages highlight a global biological event corresponding to the explosion of smooth-shaped ostracods, represented by the Family Cytherellidae. The Cytherellid Event is related to the biotic crisis of the Cenomanian-Turonian transition (OAE2) and related to the increased temperature of sea water and oxygen depleted conditions in the bottom.

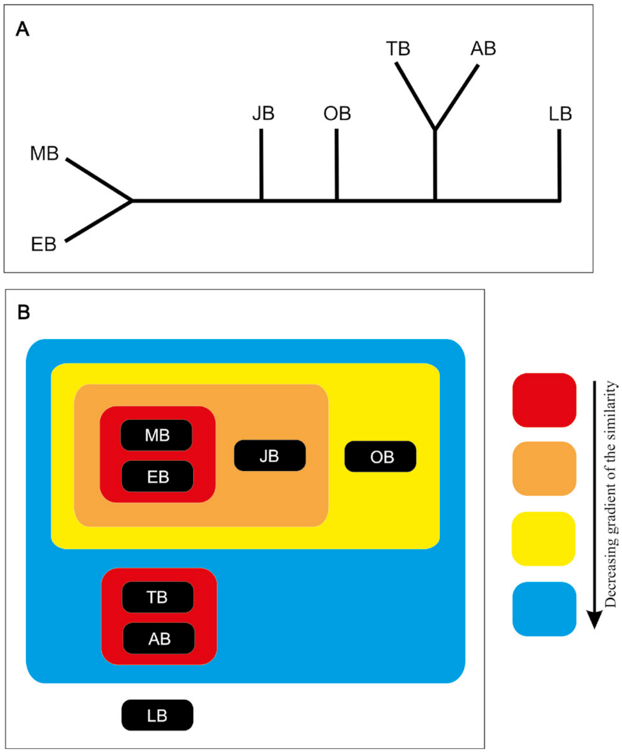

Figure 12.—A. Reconstituted phenogramm for Cenomanian-Turonian transition. B. Hierarchical association diagram between basins.

Furthermore, the calculation of ostracod similarity and distance indices by the BG-Index allowed the comparison of seven regions belonging to palaeobiogeographic provinces of North Africa-Middle East (Gondwana palaeomargin). The results thus obtained show a general topology in the Cenomanian-Turonian transition, marked by the binary similarity between the Moroccan and Egyptian basins on the one hand and the basins of the Saharan Atlas (Algeria, Tunisia) on the other. This palaeobiogeographical topology indicates the probable existence of communication routes between some basins and the isolation of the ostracod fauna of the Lebanese Basin.

ACKNOWLEDGEMENTS

We thank the constructive comments of three reviewers (Julio Rodríguez Lázaro and two anonymous) which have improved this work. This study had the support of funding from Spanish Ministry of Economy and Competitiveness, project PID2019-105537RB-100.

References

Abed, S. (1982). Lithostratigraphie et sédimentologie du Jurassique moyen et supérieur du Djebel Amour (Atlas saharien). MSc Thesis, Université de Pau, 242 p.

Accarie, H.; Robaszynski, F.; Amédro, F.; Caron, M. & Zagrarni, M.F. (2000). Stratigraphie événementielle au passage Cénomanien-Turonien dans le secteur occidental de la plate-forme de Tunisie centrale (Formation Bahloul, région de Kalaat Senan). Annales des Mines et de la Géologie Tunis, 40: 63-80.

Aguado, R.; Reolid, M. & Molina, E. (2016). Response of calcareous nannoplankton to the Late Cretaceous Oceanic Anoxic Event 2 at Oued Bahloul (central Tunisia). Palaeogeography, Palaeoclimatology, Palaeoecology, 459: 289-305. https://doi.org/10.1016/j.palaeo.2016.07.016

Aït Ouali, R. (1991). Le rifting des monts des Ksour au Lias: Organisation du bassin, diagenèse des assises carbonatées, place dans les ouvertures mésozoïques au Maghreb. PhD Thesis, Université Houari Boumédiene Alger, 302 p.

Aït Ouali, R. & Delfaud, J. (1995). Les modalités d'ouverture du bassin des Ksour au Lias dans le cadre du «rifting» jurassique au Maghreb. Comptes Rendus Academie Sciences, Paris, 320: 773-778.

Al-Abdul Razzaq, S.K. (1979). Glenocythere, a new ostracode genus from the Hamadi Formation (Cretaceous) of Kuwait. Journal of Paleontology, 53: 920-930.

Aly, M.F. & Abdel-Gawad, G.I. (2001). Upper Cenomaniane Lower Turonian ammonites from north and central Sinai, Egypt. El-Minia Science Bulletin, 13: 17-60.

Aly, M.F.; Smadi, A. & Abu Azzam, H. (2008). Late Cenomanian-Early Turonian ammonites of Jordan. Revue de Paléobiologie, 27: 43-71.

Amédro, A.; Accarie, H. & Robaszynski, F. (2005). Position de la limite Cénomanien-Turonien dans la Formation Bahloul de Tunisie centrale: apports intégrés des ammonites et des isotopes du carbone ($\delta^{13}C$). Eclogae Geologicae Helvetiae, 98: 151-167. https://doi.org/10.1007/s00015-005-1158-5

Andreu, B. (1989). Le Crétacé moyen de la transversale Agadir-Nador (Maroc): précisions stratigraphiques et sédimentologiques. Cretaceous Research, 10: 49-80. https://doi.org/10.1016/0195-6671(89)90029-3

Andreu, B. (1991). Les ostracodes du Crétacé moyen (Barrémien à Turonien), le long d'une transversale Agadir-Nador (Maroc). PhD Thesis, Touluse 3, 756 p.

Andreu, B. (2002). Cretaceous ostracode biochronology of Morocco. Eclogae Geologicae Helvetiae, 95: 133-152.

Andreu, B. & Bilotte, M. (2006). Ostracodes du Cenomanien supérieur et du Turpnien de la zone sous-pyrénéenne orientale (Corbières méridionales, SE France). Systématique, biostratigrahie, paléoécologie et paléobiogéographie. Revue de Micropaléontologie, 49: 55-73. https://doi.org/10.1016/j.revmic.2005.12.001

Andreu, B.; Lebedel, V.; Wallez, M.J.; Lézin, C. & Ettachfini, M. (2013). The upper Cenomanian lower Turonian carbonate platform of the Preafrican Trough, Morocco: Biostratigraphic, paleoecological and paleobiogeographical distribution of ostracods. Cretaceous Research, 45: 216-246. https://doi.org/10.1016/j.cretres.2013.04.005

Andreu, B. & Tronchetti, G. (1996). Ostracodes et foraminifères du Crétacé supérieur du synclinal d'El Koubbat. Moyen Atlas. Maroc: biostratigraphie, paléoenvironnements, paléobiogéographie. Systématique des ostracodes. Geobios, 29: 45-71. https://doi.org/10.1016/S0016-6995(96)80071-4

Aquit, M.; Kuhnt, W.; Holbourn, A.; Chellai, E.H.; Stattegger, K.; Kluth, O. & Jabour, H. (2013). Late Cretaceous palleoenvironmental evolution of the Tarfaya Atlantic coastal Basin, SW Morocco. Cretaceous Research, 45: 288-305. https://doi.org/10.1016/j.cretres.2013.05.004

Athersuch, J. (1988). The Biostratigraphy of Cretaceous Ostracods from Oman. Developments in Palaeontology and Stratigraphy, 11: 1187-1206. https://doi.org/10.1016/S0920-5446(08)70249-8

Ayoub-Hannaa, W.; Huntley, J.W. & Fürsich, F.T. (2013). Significance of Detrended Correspondence Analysis (DCA) in palaeoecology and biostratigraphy: A case study from the Upper Cretaceous of Egypt. Journal of African Earth Sciences, 80: 48-59. https://doi.org/10.1016/j.jafrearsci.2012.11.012

Babinot, J.F. (1980). Les ostracodes du Crétacé supérieur de Provence: systématique, biostratigraphie, paléoécologie, paléogéographie. Travaux du Laboratoire de Géologie Historique et Paléontologie, 10: 1-624.

Babinot, J.F. & Basha, S.A. (1985). Ostracods from the Early Cenomanian of Jordan. A preliminary report. Geobios, 18: 257-262. https://doi.org/10.1016/S0016-6995(85)80019-X

Barroso-Barcenilla, F.; Pascual, A.; Peyrot, D. & Rodríguez-Lazaro, J. (2011). Integrated biostratigraphy and chemostratigraphy of the upper Cenomanian and lower Turonian succession in Puentedey, Iberian Trough, Spain. Proceedings of Geologists' Association, 122: 67-81. https://doi.org/10.1016/j.pgeola.2010.11.002

Bassiouni, M.A.A. (2002). Mid-Cretaceous (Aptian-Early Turonian) ostracoda from Sinai. Neue Paläontologische Abhandlungen, 5: 1-123.

Bassoullet, J.P. (1973). Contribution à l'étude stratigraphique du Mésozoïque de l'Atlas saharien occidental (Algérie). PhD Thesis, Univ. Pierre et Marie Curie Paris, 477 p.

Bassoullet, J.P. & Damotte, R. (1969). Quelques ostracodes nouveaux du Cénomanien-Turonien de l’Atlas saharien occidental (Algérie). Revue de Micropaléontologie, 3: 130-144.

Bauer, J.; Kuss, J. & Steuber, T. (2002). Platform environments, microfacies and systems tracts of the Upper Cenomanian - Lower Santonian of Sinai, Egypt. Facies, 47: 1-25. https://doi.org/10.1007/BF02667703

Benadla, M. (2019). Le passage Cénomanien-Turonien dans l’Atlas Saharien algérien: Sédimentologie, Biostratigraphie et Géochimie. PhD Thesis, University of Tlemcen, 184 p.

Benadla, M.; Reolid, M.; Marok, A. & El Kamali, N. (2018). The Cenomanian-Turonian transition in the carbonate platform facies of the Western Saharan Atlas (Rhoundjaïa Formation, Algeria). Journal of Iberian Geology, 44: 405-429. https://doi.org/10.1007/s41513-018-0070-6

Bergue, C.T.; Fauth, G.; Coimbra, J.C.; Ahmad, F.Y.; Smadi, A. & Farouk, S. (2016). The late Albian-early Cenomanian ostracodes from Naur formation, Jordan. Revista Brasileira de Paleontologia, 19: 195-210. https://doi.org/10.4072/rbp.2016.2.04

Bettahar, A. (2009). Les accidents majeurs de l’Atlas saharien central et les structures associées. PhD Thesis, University of Science and Technology Houari Boumediene, 210 p.

Bettahar, A.; Ait Ouali, R. & Beche, A. (2007). Etude de la région de Djebel Er-Radjel à déformation polyphasée avec mise en évidence d’une inversion tectonique (Atlas saharien central, Algérie). Bulletin Service géologique National, 18: 43-56.

Bismuth, H.; Donze, P.; Lefevre, J. & Saint-Marc, P. (1981). Nouvelles espèces d’ostracodes dans le Crétacé Moyen et supérieur du Djebel Semmama (Tunisie du Centre-Nord). Cahiers de Micropaléontologie, 3: 51-69. https://doi.org/10.1016/0195-6671(82)90018-0

Bonnet, L.; Andreu, B.; Rey, J.; Cubaynes, R.; Ruget, C.; N’Zaba-Makaya, O. & Brunel, F. (1999). Fluctuations of environmental factors as seen by means of statistical analyses in micropaleontological assemblages from a Liassic Series. Micropaleontology, 45: 399-417. https://doi.org/10.2307/1486122

Boukhary, M.; Eissa, R. & Kerdany, M. (1977). Some ostracod species from the Galala Formation, western coast of the Gulf of Suez, Egypt. Proceedings Egyptian Academy Sciences Cairo, 30: 155-161.

Boukhary, M.; Morsi, A.M.; Eissa, R. & Kerdany, M. (2009). Late Cenomanian ostracode faunas from the area south of Ain Sukhna, werstern side of the Suez, Egypt. Geologica Croatica, 62: 19-30. https://doi.org/10.4154/GC.2009.02

Bracene, R. (2001). Géodynamique du nord de l’Algérie: impact sur l’exploration pétrolière. PhD Thesis, University of Cergy Pontoise, 101 p.

Bryant, R. & Belanger, C.L. (2023). Spatian heterogeneity in benthic foraminiferal assemblages tracks regional impacts of paleoenvironmental change across Cretaceous OAE2. Paleobiology, 1-23, https://doi.org/10.1017/pab.2022.47

Busson, G.; Dhondt, A.; Amédro, F.; Néraudeau, D. & Cornée, A. (1999). La grande transgression du Cénomanien supérieur-Turonien inférieur sur la Hamada de Tinrhert (Sahara algérien): Datations biostratigraphiques, environnements de dépôt et comparaison d’un témoin épicratonique avec les séries contemporaines à matière organique du Maghreb. Cretaceous Research, 20: 29-46. https://doi.org/10.1006/cres.1998.0137

Caron, M.; Dall’ Agnolo, S.; Accarie, H.; Barrera, E.; Kauffman, E.G.; Amédro, F. & Robaszynski, F. (2006). High-resolution stratigraphy of the Cenomanian-Turonian boundary interval at Pueblo (USA) and Wadi Bahloul (Tunisia): stable isotope and bio-events correlation. Geobios, 39: 171-200. https://doi.org/10.1016/j.geobios.2004.11.004

Coiffait, P.E.; Coiffait, B.; Jaeger, J.J. & Mahboubi, M. (1984). Un nouveau gisement à mammifères fossiles d’âge Eocène supérieur sur le versant sud des Nementchas (Algérie orientale): découverte des plus anciens rongeurs d’Afrique. Comptes Rendus Academie Sciences Paris, 299: 893-898.

Damotte, R. & Freytet, P. (1974). Contribution à la connaissance du Cénomanien du Massif de Fontfroide (Aude, France): Etude des Ostracodes. Revista Española de Micropaleontología, 2: 201-207.

Damotte, R. & Saint-Marc, P. (1972). Contribution a la connaissance des ostracodes Crétacé du Liban. Revista Española de Micropaleontología, 4: 273-296.

Delfaud, J. (1975). Les grès des Ksour: un delta de plate-forme stable. XIème Congrès International de Sédimontologie, Nice, 159-162.

Delfaud, J. (1986). Organisation scalaire des événements sédimentaires majeurs autour de la Mésogée durant le Jurassique et le Crétacé. Conséquences pour les associations biologiques. Bulletin des centres de recherches exploration-Production Elf-Aquitaine, 10 (2): 509-535.

Depêche, F. (1984). Les ostracodes d’une plate-forme continentale au Jurassique. Recherches sur le Bathonien du Bassin parisien. PhD Thesis, University Pierre et Marie Curie, Paris, 325 p.

Elderbak, K.; Leckie, R.M. & Tibert, N.E. (2014). Paleoenvironmental and paleoceanographic changes across the Cenomanian-Turonian Boundary Event (Oceanic Anoxic Event 2) as indicated by foraminiferal assemblages from the eastern margin of the Cretaceous Western Interior Sea. Palaeogeography, Palaeoclimatology, Palaeoecology, 413: 29-48. https://doi.org/10.1016/j.palaeo.2014.07.002

Elmi, S.; Alméras, Y.; Ameur, M.; Bassoullet, J.B.; Boutakiout, M.; Benhamou, M.; Marok, A.; Mekahli, L.; Mekkaoui, A. & Mouterde, R. (1998). Stratigraphic and palaeogeographic survey of the Lower and Middle Jurassic along a north-south transect in western Algeria. Mémoires Musée National Histoire Naturel Paris, 179: 145-211.

El-Nady, H.; Abu-Zied, R. & Ayyad, S. (2008). Cenomanian Maastrichtian ostracods from Gabal Arif El-Naga anticline, Eastern Sinai, Egypt. Revue de Paléobiologie, 27: 533-573.

El-Sabbagh, A.; Tantawy, A.A.; Keller, G.; Khozyem, H.; Spangenberg, J.; Adatte, T. & Gertsch, B. (2011). Stratigraphy of the Cenomanian-Turonian Oceanic Anoxic Event OAE2 in shallow shelf sequences of NE Egypt. Cretaceous Research, 32: 705-722. https://doi.org/10.1016/j.cretres.2011.04.006

Erba, E. (2004). Calcareous nannofossils and Mesozoic oceanic anoxic events. Marine Micropaleontology, 52: 85-106. https://doi.org/10.1016/j.marmicro.2004.04.007

Erba, E.; Bottini, C. & Faucher, G. (2013). Cretaceous large igneous provinces: the effects of submarine volcanism on calcareous nannoplankton. Mineralogical Magazine, 77: 1044.

Erbacher, J. & Thurow, J. (1997). Influence of oceanic anoxic events on the evolution of mid Cretaceous radiolaria in the North Atlantic and western Tethys. Marine Micropaleontology, 30: 139-158. https://doi.org/10.1016/S0377-8398(96)00023-0

Escarguel, G. (2001). BG-Index version 1.1β. Programme et notice d'utilisation. Laboratoire de Paléontologie, Université Claude Bernard.

Ettachfini, M. (2006). La transgression au passage du Cénomanien au Turonien sur le domaine atlasique marocain. Stratigraphie intégrée et relation avec l'évenement océanique global. PhD Thesis, University Chouaïb Doukkali, 299 p.

Ettachfini, M. & Andreu, B. (2004). Le Cénomanien et le Turonien de la Plate-forme Préafricaine du Maroc. Cretaceous Research, 25: 277-302. https://doi.org/10.1016/j.cretres.2004.01.001

Ettachfini, M.; Souhel, A.; Andreu, B. & Caron, M. (2005). La limite Cénomanien -Tutronien dans le Haut Atlas central, Maroc. Geobios, 38: 57-68. https://doi.org/10.1016/j.geobios.2003.07.003

Farouk, S.; Jain, S.; Shabaan, M.; Ahmad, F.; Salhi, I.; Elamri, Z.; El-Kahtany, K.; Zaky, A.S. & Abu Sham, A. (2022). High resolution upper Cenomanian to Turonian paleoenvironmental changes: Inferences from calcareous nannofossils at the Oued Ettalla section (Central Tunisia). Marine Micropaleontology, 175: 102151. https://doi.org/10.1016/j.marmicro.2022.102151

Friedrich, O.; Erbacher, J. & Mutterlose, J. (2006). Paleoenvironmental changes across the Cenomanian/Turonian Boundary Event (Oceanic Anoxic Event 2) as indicated by benthic foraminifera from the Demerara Rise (ODP Leg 207). Revue de Micropaléontologie, 49: 121-139. https://doi.org/10.1016/j.revmic.2006.04.003

Galmier, D. (1972). Photogéologique de la région d'Aïn Séfra (Algérie). Bulletin Service Géologique Algérie, 42: 1-177.

Gebhardt, H.; Friedrich, O.; Schenk, B.; Fox, L.; Hart, M. & Wagreich, M. (2010). Paleoceanographic changes at the northern Tethyan margin during the Cenomanian-Turonian Oceanic Anoxic Event (OAE-2). Marine Micropaleontology, 77: 25-45. https://doi.org/10.1016/j.marmicro.2010.07.002

Gebhardt, H.; Kuhnt W. & Holbourn, A. (2004). Foraminiferal response to sea level change, organic flux and oxygen deficiency in the Cenomanian of the Tarfaya Basin, southern Morocco. Marine Micropaleontology, 53: 133-157. https://doi.org/10.1016/j.marmicro.2004.05.007

Gertsch, B.; Keller, G.; Adatte, T.; Berner, Z.; Kassab, A.S.; Tantawy, A.A.A.; El-Sabbagh, A.M. & Stueben, D. (2010). Cenomanian-Turonian transition in a shallow water sequence of the Sinai, Egypt. International Journal of Earth Sciences, 99: 165-182. https://doi.org/10.1007/s00531-008-0374-4

Glintzboeckel, C. & Magné, J. (1959). Répartition des microfaunes à plancton et à Ostracodes dans le Crétacé supérieur de la Tunisie et de l'Est algérien. Revue de Micropaléontologie, 5: 53-59.

Grekoff, M. (1969). Sur la valeur stratigraphique et les relations paléogéographiques des quelques ostracodes du Crétacé, du Paléocène et de l'Eocène inférieur d'Algérie orientale. Proceedings of the 3rd African Micropaleontological Coloquium, Cairo, 227-248.

Grosdidier, E. (1973). Association d'Ostracodes du Crétacé d'Iran. Revue Institute Français du Pétrole, 28 (2): 131-169.

Grosheny, D.; Chikhi-Aouimeur, F.; Ferry, S.; Benkherouf-Kechid, F.; Jati, M.; Atrops, F. & Redjimi-Bourouiba,

W. (2008). The Upper Cenomanian-Turonian (Upper Cretaceous) of the Saharan Atlas (Algeria). Bulletin Société Géologique France, 179: 593-603. https://doi.org/10.2113/gssgfbull.179.6.593

Grosheny, D.; Ferry, S.; Jati, M.; Ouaja, M.; Bensalah, M.; Atrops, F.; Chikhi-Aouimeur, F.; Benkherouf-Kechid, F.; Negra, H. & Aït Salem, H. (2013). The Cenomanian-Turonian boundary on the Saharan Platform (Tunisia and Algeria). Cretaceous Research, 42: 66-84. https://doi.org/10.1016/j.cretres.2013.01.004

Guillemot, J. & Estorges, P. (1981). Notice de la carte de Brézina au 1/200000. Direction de la Géologie, Direction des Mines et de la Géologie, Ministère de l'Industrie Lourde, Algérie, 45 p.

Guiraud, R. (1990). Evolution post-triasique de l'avant-pays de la chaîne alpine en Algérie d'après l'étude du bassin du Hodna et des régions voisines. Geological Survey of Algeria, Office National de la Geologie, 259 p.

Hallam, A. (1992). Phanerozoic sea level changes. Columbia Press, New York, 266 p.

Hammer, Ø., Harper, D. A. T., & Ryan, P. D. (2001). PAST-palaeontological statistics, ver. 1.89. Palaeontologia Electronica, 4 (1): 1-9.

Hardas, P. & Mutterlose, J. (2007). Calcareous nannofossil assemblages of Oceanic Anoxic Event 2 in the equatorial Atlantic: Evidence of a eutrophication event. Marine Micropaleontology, 66: 52-69. https://doi.org/10.1016/j.marmicro.2007.07.007

Harket, M. & Delfaud, J. (2000). Genèse des séquences sédimentaires du Crétacé supérieur des Aurès (Algérie). Rôle de l'eustatisme, de la tectonique, de la subsidence : une mise au point. Comptes Rendus Academie Sciences de Paris, 330: 785-792. https://doi.org/10.1016/S1251-8050(00)00229-9

Hataba, H. & Ammar, G. (1990). Comparative stratigraphic study on the Upper Cenomanian - Lower Senonian sediments between the Gulf of Suez and Western Desrt, Egypt. EGPC 10th Exploration-Production Conference, 1-16.

Hewaidy, A.A. & Morsi, A.M. (2001). Lower Cretaceous (Aptian-Albian) Foraminifera and Ostracoda from northern Sinai, Egypt. Egyptian Journal of Paleontology, 1: 229-252.

Horne, D.J.; Cohen, A. & Martens, K. (2002). Taxonomy, morphology and biology of Quaternary and living Ostracoda. In: Holmes, J.A., Chivas, A.R. (Eds.), The Ostracoda: Applications in Quaternary Research. AGU Geophysical Monograph Series, 131: 5-36. https://doi.org/10.1029/131GM02

Horne, D.J.; Brandao, S.N. & Slipper, I.J. (2011). The Platycopid signal deciphered: responses of ostracod taxa to environmental change during the Cenomanian-Turonian boundary event (Late cretaceous) in SE England. Palaeogeography, Palaeoclimatology, Palaeoecology, 308: 304-312. https://doi.org/10.1016/j.palaeo.2011.05.034

Huber, B.T.; Norris, R.D. & McLeod, K.G. (2002). Deep-sea paleotemperature record of extreme warmth during the Cretaceous. Geology, 30: 123-126. https://doi.org/10.1130/0091-7613(2002)030<0123:DSPROE>2.0.CO;2

Ismail, A.A. (1999). Aptian-Turonian ostracods from Northern Sinai, Egypt. Egyptian Journal of Geology, 43: 293-315.

Ismail, A.A. (2001). Correlation of cenomanian-Turonian ostracods of Gebel Shabraweet with their counterpart in Egypt, Nort Africa and the Middle East. Neues Jahrbush Geologische Paläontologische Monatshefte, 9: 513-533. https://doi.org/10.1127/njgpm/2001/2001/513

Ismail, A.A.; Hussein-Kamel, Y.F.; Boukhary, M. & Ghandour, A.A. (2009). Late Cenomanian-Early Turonian foraminifera from Eastern Desert, Egypt. Micropaleontology, 55: 396-412. https://doi.org/10.47894/mpal.55.4.05

Jarvis, I.; Carson, G.A.; Cooper, M.K.E.; Hart, M.B.; Leary, P.N.; Tocher, B.A.; Horne, D. & Rosenfeld, A. (1988). Microfossil assemblages and the Cenomanian-Turonian (late Cretaceous) oceanic anoxic event. Cretaceous Research, 9: 3-103. https://doi.org/10.1016/0195-6671(88)90003-1

Jati, M.; Grosheny, D.; Ferry, S.; Masrour, M.; Aoutem, M.; Içame, N.; Gauthier-Lafaye, F. & Desmares, D. (2010). The Cenomanian-Turonian boundary event onthe Moroccan Atlantic margin (Agadir basin): Stable isotope and sequence stratigraphy. Palaeogeography, Palaeoclimatology, Palaeoecology, 296: 151-164. https://doi.org/10.1016/j.palaeo.2010.07.002

Jenkyns, H.C. (1980). Cretaceous anoxic events: from continents to oceans. Journal Geological Society London, 137: 171-188. https://doi.org/10.1144/gsjgs.137.2.0171

Jenkyns, H.C. (1997). Mesozoic anoxic events and paleoclimate. Zentralblatt für Geologie und Paläontologie, 1: 943-949.

Jolet, P.; Philip, J.; Cecca, F.; Thomel, G.; López, G.; Tronchetti, G. & Babinot, J.F. (2001). Integrated platform/basin biostratigraphy of the Upper Cenomanian-Lower Turonian in Provence (SE France). Geobios, 34: 225-238. https://doi.org/10.1016/S0016-6995(01)80063-2

Kaiho, K. & Hasegawa, T. (1994). End-Cenomanian benthic foraminiferal extinctions and oceanic dysoxic events in the northwestern Pacific Ocean. Palaeogeography, Palaeoclimatology, Palaeoecology, 111: 29-43. https://doi.org/10.1016/0031-0182(94)90346-8

Kazi-Tani, N. (1986). Evolution géodynamique de la bordure nord-africaine: le domaine intraplaque nord-algérien. Approche mégaséquentielle. PhD Thesis, University of Pau, 871 p.

Khalil, M.M. (2020). Biostratigraphy and paleobiogeographic implications of the Cenomanian-Early Turonian ostracods of Egypt. Annales de Paléontologie, 106: 102408. https://doi.org/10.1016/j.annpal.2020.102408

Kostak, M.; Cech, S.; Ulicny, D.; Sklenar, J.; Ekrt, B. & Mazuch, M. (2018). Ammonites, inoceramids and stable carbon isotopes of the Cenomanian-Turonian OAE2 interval in central Europe: Pecinov quarry, Bohemian Cretaceous Basin (Czech Republic). Cretaceous Research, 87: 150-173. https://doi.org/10.1016/j.cretres.2017.04.013

Kuroda, J.; Ogawa, N.O.; Tanimizu, M.; Coffin, M.T.; Tokuyama, H.; Kitazato, H. & Ohkouchi, N. (2007). Contemporaneous massive subaerial volcanism and late Cretaceous Oceanic Anoxic Event 2. Earth Planetary Science Letters, 256: 211-223. https://doi.org/10.1016/j.epsl.2007.01.027

Kuypers, M.M.M.; Pancost, R.D.; Nijenhuis, I.A. & Sinninghe-Damste, J.S. (2002). Enhanced productivity led to increased organic carbon burial in the euxinic North Atlantic Basin during the late Cenomanian oceanic anoxic event. Paleoceanography, 17: 1051. https://doi.org/10.1029/2000PA000569

Lézin, C.; Andreu, B.; Ettachfini, M.; Walleez, M.-J.; Lebedel, V. & Meister, C. (2012). The upper Cenomanian-lower Turonian of the Preafrican Trough, Morocco. Sedimentary Geology, 245-246: 1-16. https://doi.org/10.1016/j.sedgeo.2011.12.003

Lüning, S.; Marzouk, A.M.; Morsi, A.M. & Kuss, J. (1998). Sequence stratigraphy of the Upper Cretaceous of central-east Sinai, Egypt. Cretaceous Research, 19: 153-196. https://doi.org/10.1006/cres.1997.0104

Majoran, S. (1989). Mid-Cretaceous Ostracoda of northeastern Algeria. Fossils Strata, 27: 1-67.

Marok, A.; Sebane, A. & Bensalah, M. (2009). Les événements anoxiques du Mésozoïque dans quelques bassins nord algériens: Résultats préliminaires. Conférences sur l'Exploration dans le Nord de l'Algérie: Perspectives et Défis, Alger, 27-28.

Mebarki, K.; Sauvagnat, J.; Benyoucef, M.; Zaoui, D.; Benachour, H-B.; Mohammed, A.; Mahboubi, M. & Bensalah, M. (2016). Cenomanian-Turonian ostracodes fron the Western Saharan Atlas and the Guir Basin (SE Algeria): systematic, biostratigraphy and paleobiogeography. Revue de Paleobiologie, 35: 249-277.

Mekahli, L. (1998). Evolution des Monts des Ksour (Algérie) de l'Héttangien au Bajocien. Biostratigraphie, sédimentologie, paléogéographie et stratigraphie séquentielle. Documents Laboratoire Géologie Lyon, 147: 319 p.

Momani, M.M. (2021). Petrographical and Geochemical Analyses of the Cenomanian-Turonian Oil Shale Successions in Ajloun, Northern of Jordan. PhD Thesis, University of Yarmouk, 79 p.

Monnet, C. (2009). The Cenomanian-Turonian boundary mass extinction (Late Cretaceous): New insights from ammonoid biodiversity patterns of Europe, Tunisia and the Western Interior (North America). Palaeogeography, Palaeoclimatology, Palaeoecology, 282: 88-104. https://doi.org/10.1016/j.palaeo.2009.08.014

Monteiro, F.M.; Pancost, R.D.; Ridwell, A. & Donnadieu, Y. (2012). Nutrients as the dominant control on the spread of anoxia and euxinia across the Cenomanian-Turonian oceanic anoxic event (OAE2): model-data comparison. Paleoceanography, 27 (4): PA4209. https://doi.org/10.1029/2012PA002351

Morsi, A.M. & Bauer, J. (2001). Cenomanian ostracods from Sinai Peninsula, Egypt. Revue de Paléobiologie, 20: 377-414.

Morsi, A.M. & Wendler, J.E. (2010). Biostratigraphy, palaeoecology and palaeogeography of the Middle Cenomanian-Early Turonian Levant Platform in Central Jordan based on ostracods. Geological Society Special Publication, 341: 187-201. https://doi.org/10.1144/SP341.9

Nagm, E. (2009). Integrated stratigraphy, palaeontology and facies analysis of the Cenomanian-Turonian (Upper Cretaceous) Galala and Maghra El Hadida Formations of the Western Wadi Araba, Eastern Desert, Egypt. PhD Thesis, University of Würzburg, 213 p. https://doi.org/10.1127/0078-0421/2010/0002

Nagm, E.; Wilmsen, M.; Aly, M.F. & Hewaidy, A. (2010). Upper Cenomanian-Turonian (Upper Cretaceous) ammonoids from the western Wadi Araba, Eastern Desert, Egypt. Cretaceous Research, 31: 473-499. https://doi.org/10.1016/j.cretres.2010.05.008

Nagm, E.; Farouk, S. & Ahmed, F. (2017). The Cenomanian-Turonian boundary in Jordan: Ammonite biostratigraphy and faunal turnover. Geobios, 50: 37-47. https://doi.org/10.1016/j.geobios.2016.11.002

Nagm, E.; Jain, S.; Mahfouz, K.; El Sabbagh, A. & Abu Shama, A. (2021). Biotic response to the latest Cenomanian drowning and OAE2: A case study from the Eastern Desert of Egypt. Proceedings Geologists' Association, 132: 70-92. https://doi.org/10.1016/j.pgeola.2020.10.001

Naili, H.; Belhadj, Z.; Robaszynski, F. & Caron, M. (1995). Présence de roches mère à faciès Bahloul vers la limite Cénomanien-Turonien dans la région de Tébessa (Algérie orientale). Notes du Service Géologique Tunisie, 61: 19-32.

Negra, M.H.; Zagrarni, M.F.; Hanini, A. & Strasser, A. (2011). The filament event near the Cenomanian-Turonian boundary in Tunisia: filament origin and environmental signification. Bulletin de la Société Géologique de France, 182: 507-519. https://doi.org/10.2113/gssgfbull.182.6.507

Neufville, E.M.H. (1973). Ostracoda from the Ezu-Akshale (Turonian, Cretaceous), Nkalagu, Nigeria. Bulletin of the Geological Institution of the University of Uppsala, 4: 44-51.

Norris, R.D.; Bice, K.L.; Magno, E.A. & Wilson, P.A. (2002). Jiggling the tropical thermostat in the Cretaceous hothouse. Geology, 30: 299-302. https://doi.org/10.1130/0091-7613(2002)030<0299:JTTTIT>2.0.CO;2

N'Zaba-Makaya, O.; Andreu, B.; Brunel, F.; Mouterde, R.; Rey, J. & Rocha, R.B. (2003). Biostratigraphie et paléoécologie des peuplements d'ostracodes dans le Domérien du Bassin Lusitanien, Portugal. Ciências da Terra, 15: 21-44.

Piovesan, E.K.; Cabral, M.C.; Colin, J.-P.; Fauth, G. & Bergue, C.T. (2014). Ostracodes from the Upper Cretaceous deposits of the Potiguar Basin, Northeastern Brazil: taxonomy, paleoecology and paleobiogeography, part 1: Turonian. Carnets de Géologie, 14: 211-252. https://doi.org/10.4267/2042/54003

Pogge von Strandmann, P.A.E.; Jenkyns, H.C. & Woodfine, R.G. (2013). Lithium isotope evidence for enhanced weathering during Oceanic Anoxic Event 2. Nature Geosciences, 6: 668-672 https://doi.org/10.1038/ngeo1875

Posenato, R.; Frijia, G.; Morsilli, M.; Moro, A.; Del Viscio, G. & Mezfa, A. (2020). Paleoecology and proliferation of the bivalve Chondrodonta joannae (Choffat) in the upper Cenomanian (Upper Cretaceous) Adriatic Carbonate Platform of Istria (Croatia). Palaeogeography, Palaeoclimatology, Palaeoecology, 548: 109703. https://doi.org/10.1016/j.palaeo.2020.109703

Prauss, M.L. (2012). The Cenomanian/Turonian Boundary Event (CTBE) at Tarfaya, Morocco, northwest Africa: Eccentricity controlled water column stratification as major factor for total organic carbon (TOC) accumulation: Evidence from marine palynology. Cretaceous Research, 37: 246-260. https://doi.org/10.1016/j.cretres.2012.04.007

Reolid, M. (2020). Microfossil assemblages and geochemistry for interpreting the incidence of the Jenkyns Event (early Toarcian) in the south-eastern Iberian palaeomargin (External Subbetic, SE Spain). Journal of Micropalaeontology, 39: 233-258. https://doi.org/10.5194/jm-39-233-2020

Reolid, M. & Ainsworth, N.R. (2022). Changes in benthic microfossil assemblages before, during and after the eary Toarcian biotic crisis in the Portland-Wight Basin (Kerr McGee 97/12-1 well, offshore southern England). Palaeogeography, Palaeoclimatology, Palaeoecology, 599: 111044. https://doi.org/10.1016/j.palaeo.2022.111044

Reolid, M.; Rodríguez-Tovar, F.J.; Marok, A. & Sebane, A. (2012). The Toarcian Oceanic Anoxic Event in the Western Saharan Atlas, Algeria (North African Paleomargin): role of anoxia and productivity. Geological Society of America Bulletin, 124: 1646-1664. https://doi.org/10.1130/B30585.1

Reolid, M.; Sánchez-Quiñónez, C.A.; Alegret, L. & Molina, E. (2015). Palaeoenvironmental turnover across the Cenomanian-Turonian transition in Oued Bahloul, Tunisia: foraminifera and geochemical proxies. Palaeogeography, Palaeoclimatology, Palaeoecology, 417: 491-510. https://doi.org/10.1016/j.palaeo.2014.10.011

Reolid, M.; Sánchez-Quiñónez, C.A.; Alegret, L. & Molina, E. (2016). The biotic crisis across the Oceanic Anoxic Event 2: Palaeoenvironmental inferences based on foraminifera and geochemical proxies from the South Iberian Palaeomargin. Cretaceous Research, 60: 1-27. https://doi.org/10.1016/j.cretres.2015.10.011

Rerbal, L. (2008). Le Crétacé supérieur du Djebel El Kohol (Atlas saharien, Algérie). MsC Thesis, University of Tlemcen, 59 p.

Robaszynski, F. (1989). L'événement à l'échelle globale pendant la partie moyenne du Crétacé. Geobios Mémoire Spécial, 11: 311-319. https://doi.org/10.1016/S0016-6995(89)80067-1

Robaszynski, F. & Caron, M. (1995). Foraminifères planctoniquesdu Crétacé: Commentaire de la zonation Europe-Méditerranée. Bulletin de la Société Géologique France, 166: 681-692.

Robaszynski, F.; Zagrararni, M.F.; Caron, M. & Amedro, F. (2010). The global bio-event at the Cenomanian-Turonien transition in the reduced Bahloul Formation of Bou Ghanem (central Tunisia). Cretaceous Research, 31: 1-15. https://doi.org/10.1016/j.cretres.2009.07.002

Ruault-Djerrab, M.; Ferré, B.; Kechid-Benkherouf, F. & Djerrab, A. (2012). Etude micropaléontologique du Cénomano-Turonien dans la région de Tébessa (NE Algérie): implications paléoenvironnementales et recherche de l'empreinte de l'OAE2. Revue Paléobiologie, 31: 127-144.

Ruault-Djerrab, M.; Kechid-Benkherouf, F. & Djerrab, A. (2014). Données paléoenvironnementales sur le Vraconnien/Cénomanien de la région de Tébessa (Atlas Saharien, nord-est Algérie). Caractérisation de l'OAE2. Annales de Paléontologie, 100: 343-359. https://doi.org/10.1016/j.annpal.2014.03.002

Salmouna, D.J.; Chaabani, F.; Dhahri, F.; Mzoughi, M.; Salmouna, A. & Zijlstra, H.B. (2014). Lithostratigraphic analysis of the Turonien-Coniacian Bireno and Douleb carbonate Members in Jebels Berda and Chemsi, Gafsa basin, central-southern Atlas of Tunisia. Journal of African Earth Sciences, 100: 733-754. https://doi.org/10.1016/j.jafrearsci.2014.07.025

Schlanger, S.O.; Arthur, M.A.; Jenkyns, H.C. & Scholle, P.A. (1987). The Cenomanian- Turonian oceanic anoxic event, I. Stratigraphy and distribution of organic-rich beds and the marine δ13C excursion. Geologival Society Special Publication, 26: 371-399. https://doi.org/10.1144/GSL.SP.1987.026.01.24

Schulze, F.; Marzouk, A.M.; Bassiouni, M.A.A. & Kuss, J. (2004). The late Albian-Turonian carbonate platform succession of west-central Jordan: stratigraphy and crisis. Cretaceous Research, 25: 709-737. https://doi.org/10.1016/j.cretres.2004.06.008

Shahin, A. (1991). Cenomanian-Turonian ostracods from Gebel Nezzazat, southwestern Sinai, Egypt, with observations on δ13C values and the Cenomanian/Turonian boundary. Journal of Micropalaeontology, 10: 133-155. https://doi.org/10.1144/jm.10.2.133

Shahin, A. & Elbaz, S. (2013a). Cenomanian-Early Turonian of the shallow marine carbonate platform sequence at west central Sinai: Biostratigraphy, paleobathymetry and paleobiogeography. Revue de Micropaléontologie, 56: 103-126. https://doi.org/10.1016/j.revmic.2013.04.004

Shahin, A. & Elbaz, S.M. (2013b). Cenomanian-Early Turonian Ostracoda of the shallow marine carbonate platform sequence at west central Sinai: Biostratigraphy, paleobathymetry and paleobiogeography. Revue de Micropaléontologie 56: 103-126. https://doi.org/10.1016/j.revmic.2013.04.004

Shahin, A. & Elbaz, S. (2021). Early-Middle Cenomanian foraminifera and ostracods from BB-80-1 well, Gulf of Suez, Egypt: Biostratigraphy, palaeoecology, and palaeobiogeographic significance. Geological Journal, 56: 3745-3770. https://doi.org/10.1002/gj.4131

Shahin, A.; Kora, M. & Semiet, A. (1994). Cenomanian ostracods from West Central Sinai, Egypt. Mansoura University Science Bulletin, 21: 33-102.

Slami, R.; Ferré, B. & Benkherouf-Kechid, F. (2022). Cenomanian ostracods (Crustacea) of Djebel Sabaoune (Batna, Algeria): Specific assemblage and significance. Journal of African Earth Sciences, 193: 104604. https://doi.org/10.1016/j.jafrearsci.2022.104604

Takahashi, A. (2005). Responses of inoceramid bivalves to environmental disturbances across the Cenomanian/Turonian boundary in the Yezo forearc basin, Hokkaido, Japan. Cretaceous Research, 26: 567-580. https://doi.org/10.1016/j.cretres.2005.02.006

Tchenar, S.; Ferré, B.; Adaci, M.; Zaoui, D.; Benyoucef, M.; Bensalah, M. & Kentri, T. (2020). Incidences de l'Évènement Anoxique Océanique II sur l'évolution des ostracodes des dépôts cénomano-turoniens du bassin du Tinrhert (SE Algérie). Carnets de Géologie, 20 (08): 145. https://doi.org/10.4267/2042/70792

Touir, J.; Mechi, C. & Ali, H.H. (2017). Changes in carbonate sedimentation and faunal assemblages in the Tunisian carbonate platform around the Cenomanian-Turonian boundary. Journal of African Earth Sciences, 129: 527-541. https://doi.org/10.1016/j.jafrearsci.2017.01.025

Turgeon, S.C. & Creaser, R.A. (2008). Cretaceous oceanic anoxic event 2 triggered by a massive magmatic episode. Nature, 454: 323-326. https://doi.org/10.1038/nature07076

Vivière, J.L. (1985). Les ostracodes du Crétacé supérieur (Vraconien à Campanien basal) de la région de Tébessa (Algérie du Nord-Est. Stratigraphie, Paléoécologie, Systématique). Mémoire Science de la Terre, University Marie Curie, Paris 85, 261.

Viviers, M.C.; Koutsoukos, E.A.M.; Da Silva-Telles, A.C. & Bengtson, P. (2000). Stratigraphy and biogeographic affinities of the late Aptian-Campanian ostracods of the Potiguar and Sergipe basins in northeastern Brazil. Cretaceous Research, 21: 407-455. https://doi.org/10.1006/cres.2000.0205

Voigt, S.; Erbacher, J.; Mutterlose, J.; Weiss, W.; Westerhold, T.; Wiese, F.; Wilmsen, M. & Wonik, T. (2008). The Cenomanian-Turonian of the Wunstorf section (North Germany): global stratigraphic reference section and new orbital time scale for Oceanic Anoxic Event 2. Newsletters on Stratigraphy, 43: 65-89. https://doi.org/10.1127/0078-0421/2008/0043-0065

Wan, X., Wignall, P.B. & Zhao, W. (2003). The Cenomanian-Turonian extinction and oceanic anoxic event: evidence from southern Tibet. Palaeogeography, Palaeoclimatology, Palaeoecology, 199: 283-298. https://doi.org/10.1016/S0031-0182(03)00543-1

Wang, J.P.; Bulot, L.G.; Taylor, K.G. & Redfern, J. (2021). Controls and timing of Cenomanian-Turonian organic enrichment and relationship to the OAE2 event in Morocco, North Africa. Marine and Petroleum Geology, 128, art. 105013. https://doi.org/10.1016/j.marpetgeo.2021.105013

Wendler, J.E.; Lehmann, J. & Kuss, J. (2010). Orbital time scale, intra-platform basin correlation, carbon isotope stratigraphy and sea-level history of the Cenomanian-Turonian Eastern Levant platform, Jordan. Geological Society Special Publication, 341: 171-186. https://doi.org/10.1144/SP341.8

Whatley, R.C. (1991). The platycopid signal: a means of detecting kenoxic events using Ostracoda. Journal of Micropalaeontology, 10: 181-183. https://doi.org/10.1144/jm.10.2.181

Whatley, R.C. (1995). Ostracoda and oceanic palaeoxygen levels. Mitteilungen aus dem Hamburgischen Zoologischen Museum und Institut, 92: 337-353.

Wilmsen, M. & Nagm, E. (2013). Sequence stratigraphy of the lower Upper Cretaceous (Upper Cenomanian-Turonian) of the Eastern Desert, Egypt. Newsletters on Stratigraphy, 46: 23-46. https://doi.org/10.1127/0078-0421/2013/0030

Yelles-Chaouche, A.K.; Aït Ouali, R.; Bracene, R.; Derder, M.E.M. & Djellit, H. (2001). Chronologie de l'ouverture du bassin des Ksour (Atlas Saharien, Algérie) au début du Mésozoïque. Bulletin Société Géologique France, 3: 285-293. https://doi.org/10.2113/172.3.285

Zaghbib-Turki, D. & Soua., M. (2013). High resolution biostratigraphy of the Cenomanian-Turonian interval (OAE2) based on planktonic foraminiferal bioevents in North-Central Tunisia. Journal of African Earth Sciences, 78: 97-108. https://doi.org/10.1016/j.jafrearsci.2012.09.014

Zagrarni, M.F.; Negra, M.H. & Amine Hanini, A. (2008). Cenomanian-Turonian facies and sequence stratigraphy, Bahloul Formation, Tunisia. Sedimentary Geology, 204: 18-35. https://doi.org/10.1016/j.sedgeo.2007.12.007

Zakhera, M.S. & Kassab, A.S. (2002). Integrated macrobiostratigraphy of the Cenomanian-Turonian transition, Wadi El-Siq, west central Sinai, Egypt. Egyptian Journal of Paleontology, 2: 219-233.

Zazoun, R.S.; Marok, A.; Samar, L.; Benadla, M. & Mezlah, H. (2015). La fracturation et les bandes de déformation dans la région d'El Kohol (Atlas Saharien Central, Algérie): analyse fractale, lois d'échelles et modèle de réseaux de fractures discrètes. Estudios Geologicos, 71: 1-23. https://doi.org/10.3989/egeol.42011.359